Numerical simulation of flow in the wet scrubber for desulfurization

Diplomová práce

Numerical simulation of flow in the wet scrubber for desulfurization

Diploma thesis

DIPLOMA THESIS ASSIGNMENT

(PROJECT, ART WORK, ART PERFORMANCE)

First name and surname:	**Gjemajl Maliqaj**
Study program:	**N2301 Mechanical Engineering**
Identification number:	**S15000595**
Specialization:	**Machine and Equipment Design**
Topic name:	**Numerical simulation of flow in the wet scrubber for desulfurization**
Assigning department:	**Department of Power Engineering Equipment**

Rules for elaboration:

The objective of thesis is to define material and physical model for numerical simulation of flow and chemical reactions in absorber for desulfurization of flue-gas, to perform numerical simulations and to compare the results with experiments or work of other authors.

It is expected to develop a 3D model, which takes into account the thermal, chemical and mechanical interaction of the flue-gas with droplets of lime suspension. It is recommended to use Ansys-Fluent or OpenFOAM software for simulations.

Structure of the thesis:

1. Literature overview.

2. Overview of mathematical models of mass transfer and multiphase flow.

3. Preparation and testing of the numerical model.

4. Numerical simulation of the wet scrubber.

5. Evaluation and discussion of the results.

Scope of graphic works: **20 pages**

Scope of work report
(scope of dissertation): **45 pages**

Form of dissertation elaboration: **printed**

Language of dissertation elaboration: **English**

List of specialized literature:

[1] CROWE, C., SOMMERFELD, M., TSUJI, Y., 2011. *Multiphase flows with droplets and particles.* **CRC Press.**

[2] Ansys Inc. 2012. *Fluent User's Guide Release 14.5*

[3] BES, A., 2005. *Dynamic Process Simulation of Limestone Calcination in Normal Shaft Kilns.* **Fakultät für Verfahrens und Systemtechnik der Otto von Guericke Universität Magdeburg.**

[4] XU, J. et al., 2010. *Numerical Study of the Effects of Flue Gas Inlet Type for the Flue Gas Desulfurization Wet Scrubber, Chemical Engineering Transactions, Volume 21.*

Tutor for dissertation: **doc. Ing. Tomáš Vít, Ph.D.**
Department of Power Engineering Equipment

Dissertation Counsellor: **Ing. Jan Novosád**
Department of Power Engineering Equipment

Date of dissertation assignment: **18 November 2015**

Date of dissertation submission: **18 February 2017**

prof. Dr. Ing. Petr Lenfeld
Dean

doc. Ing. Václav Dvořák, Ph.D.
Head of Department

Liberec, dated: 18 November 2015

Prohlášení

Byl jsem seznámen s tím, že na mou diplomovou práci se plně vztahuje zákon č. 121/2000 Sb., o právu autorském, zejména § 60 – školní dílo.

Beru na vědomí, že Technická univerzita v Liberci (TUL) nezasahuje do mých autorských práv užitím mé diplomové práce pro vnitřní potřebu TUL.

Užiji-li diplomovou práci nebo poskytnu-li licenci k jejímu využití, jsem si vědom povinnosti informovat o této skutečnosti TUL; v tomto případě má TUL právo ode mne požadovat úhradu nákladů, které vynaložila na vytvoření díla, až do jejich skutečné výše.

Diplomovou práci jsem vypracoval samostatně s použitím uvedené literatury a na základě konzultací s vedoucím mé diplomové práce a konzultantem.

Současně čestně prohlašuji, že tištěná verze práce se shoduje s elektronickou verzí, vloženou do IS STAG.

Datum: 26.05.2016

Podpis:

Annotation

The following thesis deals with wet flue-gas desulfurization (WFGD), which is a common industrial process applied mostly in fossil-fuel power plants. Due to emission of harmful pollutants such as SO_2, power plant units are required to control the amount of gaseous pollutants emitted into the atmosphere. SO_2 emissions are known to have detrimental impact on human health and the environment.

The purpose of this thesis is to numerically simulate the flow in the absorber for desulfurization of flue-gas. The objective is to define material and physical model for numerical simulation of flow and chemical reactions in absorber, to perform numerical simulations and to compare the results with experiments or work of related other authors. Since the main objective of the thesis deals with numerical simulations, it was developed a 3D model and the flow was simulated through the model by taking into account the mechanical, thermal, and chemical interactions of the flue-gas with the droplets of limestone suspension. The two-phase flow model of flue-gas and limestone slurry was modeled within the commercial CFD code Ansys Fluent 16.2. The continuous gas phase has been modeled with the Eulerian approach, while the dispersed phase with Lagrangian approach by tracking a large number of particles through the computational domain.

Key Words: *Wet flue-gas desulfurization, Wet scrubber, Two-phase flow, Numerical simulation*

Table of Contents

List of Tables

List of Figures

List of Symbols

Symbol	Name
H^+	Hydrogen ion
OH^-	Hydroxide ion
O_2	Oxygen
SO_2	Suflur dioxide
HSO_3	Bisulfite ion
H_2SO_3	Sulfurous acid
HCO_3^-	Bicarbonate ion
H_2O	Water
CO_2	Carbon dioxide
Ca^{2+}	Calcium ion
CO_3^{2-}	Carbonate
SO_4^{2-}	Sulfate ion
CaO	Calcium oxide
$CaCO_3$	Calcium carbonate
$CaSO_4$	Calcium sulfate
$CaSO_3 \cdot \frac{1}{2}H_2O$	Calcium sulfite hemi-hydrate
$CaSO_4 \cdot 2H_2O$	Calcium sulfate di-hydrate (Gypsum)
$MgCO_3 \cdot CaCO_3$	Dolomite

Subscripts

l	Substance in liquid phase
s	Substance in solid phase
g	Substance in gaseous phase
aq	Substance dissolved in water (aqueous)

Symbol	Name	Units
T	Flue gas temperature	[K]
ρ	Flue gas density	[kg/m^3]
p	Flue gas pressure	[Pa]
$\boldsymbol{g}$	Acceleration of gravity vector	[m/s^2]
$\boldsymbol{u}$	Flue gas velocity vector	[m/s]
$\boldsymbol{v}$	Droplet velocity vector	[m/s]
τ	Shear stress	[Pa]
τ^R	Reynolds stress tensor	[Pa]
i	Internal energy per unit mass	[J/kg]
α_d	Liquid phase volume fraction	[1]
α_c	Gas phase volume fraction	[1]
ω_A	Mass fraction of component A	[1]
c_d	Specific heat of slurry droplet	[J/kg · K]
$h_{1v,A}$	Latent heat of vaporization of component A	[J/kg]
$\dot{Q}_k$	Convective heat transfer between phases	[W/m^2 · K]
k_c	Continuous phase thermal conductivity	[W/m · K]
$F_{i,k}$	Sum of forces acting at the interface between the phases	[N]
D_{AB}	Binary diffusion coefficient of species A and B	[m^2/s]

List of Abbreviations

FGD	Flue-Gas Desulfurization
WFGD	Wet Flue-Gas Desulfurization
CFD	Computational Fluid Dynamics
DPM	Discrete Phase Model
RANS	Reynolds-Averaged Navier-Stokes
VOF	Volume of Fluid
L/G	Liquid to Gas ratio
OST	Open Spray Tower

Acknowledgements

I would like to express my sincere gratitude and appreciation to Doc. Ing. Tomáš Vít, PhD, for his continuous support of my MSc studies, and for the professionalism and guidance shown during my research.

I am also thankful to my thesis counsellor Ing. Jan Novosád, who helped me a lot during the finalization of the research, and provided me with great amount of valuable information regarding the thesis topics.

Also, I would like to express my greatest appreciation to the staff and friends from department of Power Engineering Equipment at Technical University of Liberec for all the great moments we had in the last two years.

Special thanks goes to Czech Technological Agency under project TACR TA04021338 for financial support.

I am also very thankful to project „SGS 21 135" with the support of the Specific University Research Grant, as provided by the Ministry of Education, Youth and Sports of the Czech Republic in the year 2016.

To my family – who always supported my decisions and gave my strength, I thank you a lot for your help.

Chapter 1: Introduction

1.1 *Background*

The reduction of environmental contaminants that contribute to smog and soot is a worldwide goal that has an increased focus in recent years. Wet flue-gas desulfurization is characterized as one of the most effective SO_2 removal techniques with low operating costs and high reliability. However, capital cost for implementation is considered high. Hence an effective optimization procedure is required to reduce these capital costs of conversion. Process improvement and optimization is a constantly ongoing effort. For this reason coal power plant units commonly use limestone slurry spray reaction to reduce SO_2 emissions into the atmosphere. Droplet size introduced into the tower is essential to ensuring maximum reduction while minimizing scale. The liquid slurry is known to have density, surface tension and viscosity values that deviates from standard water spray characteristics, which complicates process optimization. The improvements made in nozzle design and liquid atomization, in recent years, have provided the possibility of process optimization like never before. In order to improve the scrubber, nozzle characteristics and placements must be optimized to reduce the cost of the system implementation and mitigate risks of inadequate pollution reduction [1].

Computational fluid dynamics (CFD) projects for this type of application have become very useful. CFD is a numerical method used to numerically solve the fluid flow problems. Within the computational region, CFD solves the Navier-Stokes equations to obtain velocity, pressure, temperature and other quantities that may be required by a tackled problem. Recently CFD became a popular design and optimization tool with the help of commercially available software and advancing computer technology. The commercially available CFD package Ansys Fluent 16.2 (academic version) was used for the simulation.

1.2 *Historical overview of FGD process*

Methods of removing sulfur dioxide from boiler and furnace exhaust gases have been studied for over 150 years. Early ideas for flue-gas desulfurization (hereinafter referred as FGD) were established in England around 1850. With the construction of large-scale power plants in England in the 1920s, the problems associated with large volumes of coal burned from a single site began to concern the public. The first major FGD unit at a utility was installed in 1931 at *Battersea Power*

Station, owned by London Power Company. In 1935, an FGD system similar to that installed at Battersea went into service at Swansea Power Station.

Figure 1 – Batteresa Power Station, London (photo courtesy of Rexscanpic)

The third major FGD system was installed in 1938 at Fulham Power Station. These three early large-scale FGD installations were abandoned during World War II. Large-scale FGD units did not reappear at utilities until the 1970s, where most of the installations occurred in the United States and Japan [2].

"As of June 1973, there were 42 FGD units in operation, 36 in Japan and 6 in the United States, ranging in capacity from 5 MW to 250 MW. As of around 1999 and 2000, FGD units were being used in 27 countries, and there were 678 FGD units operating at a total power plant capacity of about 229 gigawatts. About 45% of the FGD capacity was in the U.S., 24% in Germany, 11% in Japan, and 20% in various other countries. Approximately 79% of the units, representing about 199 gigawatts of capacity, were using lime or limestone wet scrubbing. About 18% (or 25 gigawatts) utilized spray-dry scrubbers or sorbent injection systems" [3] [2].

1.3 Process description of FGD

There are many different types of scrubbers used for the removal of sulfur dioxide from flue-gas. All these technologies require use of an alkaline chemical reagent which will react with SO_2 and convert it to either liquid or solid waste by-product. The reagent is injected in the flue-gas by the spray nozzles located upstream of the tower or directly into the duct. This process can be classified as non-renewable or renewable.

In non-renewable process, the reagent in the scrubber is consumed in order to directly generate a by-product containing the sulfur, such as gypsum. In renewable process, the spent reagent is regenerated in a separate step to renew the reagent material for further use and to produce a separate by-product, such as elemental sulfur [4].

The most frequent classification is according to the character of the state in which the active ingredient is applied. The processes are classified as:

– *wet*, when the SO_2 is captured in a liquid or water suspension of the active absorbent;

– *dry*, when the SO_2 reacts with the active matter in a solid state;

– *semi-dry*, when the active matter is sprayed in the form of a water suspension into the hot flue gases, the water then evaporates and the product is captured in a solid state.

The limestone/gypsum wet process is the most widely used one because of its high SO_2 removal efficiency, high reliability, and low utility consumption. The semi-dry processes (typically spray dry scrubbers) are ranked second behind wet scrubbers [4].

The process of the detailed description of wet flue-gas desulfurization (WFGD) is systematically shown in the Figure 2
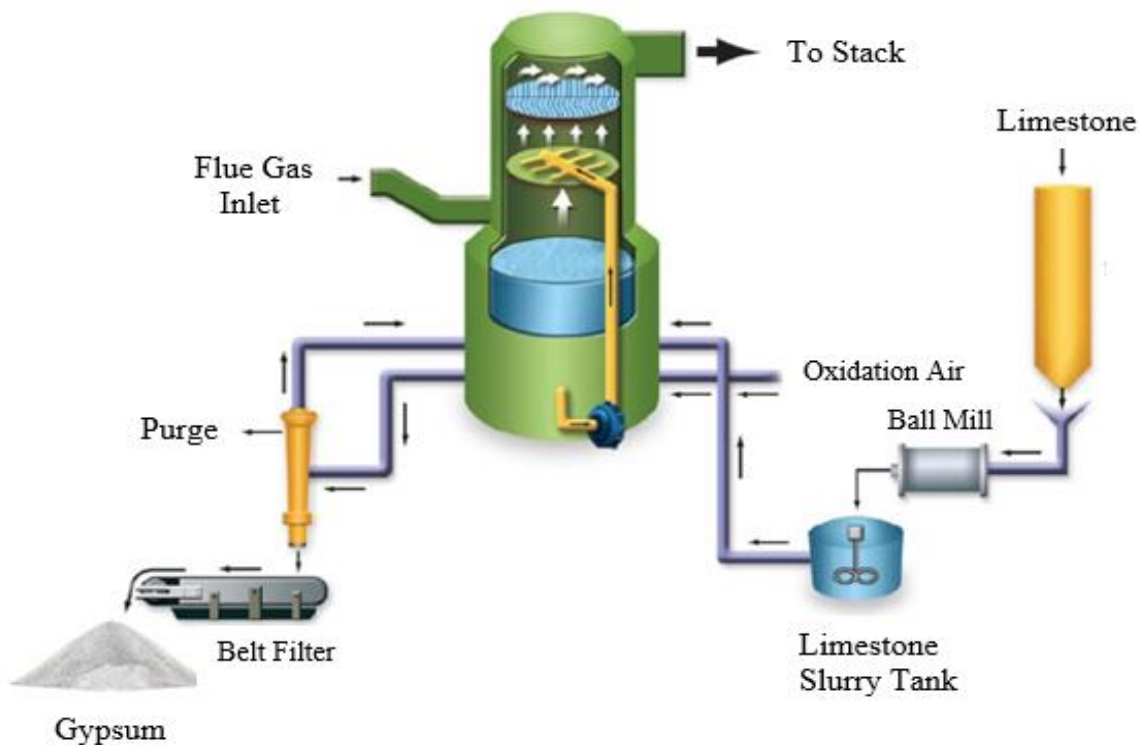
Figure 2 - Schematic of WFGD process in coal power plant units [5]

There are different equipment designs for contacting the slurry reagent with the contaminated gas stream. The capability of a particular design can be approximated from the gas stream pressure drop across the scrubber. In general, higher pressure drops indicate more aggressive contact between the liquid and the gas stream, causing smaller particles to be collected with greater efficiency. Classified by the energy use, scrubbers are divided into three groups; low energy, medium energy and high energy wet scrubbers.

1.3.1   Open spray tower

The most common wet scrubber design used today is the open spray tower (OST).

The *open spray tower* is a low energy device with pressure drop less than 1.1 kPa and is capable of efficiently removing particles greater than $5 - 10 \ \mu m$ in diameter. It consists of an open vessel with water sets of spray nozzles to distribute the scrubbing liquid. Typically the gas stream enters at the bottom and passes upwards through the sprays. This is referred as counter-current operation [6]. The described process is shown in the Figure 3.
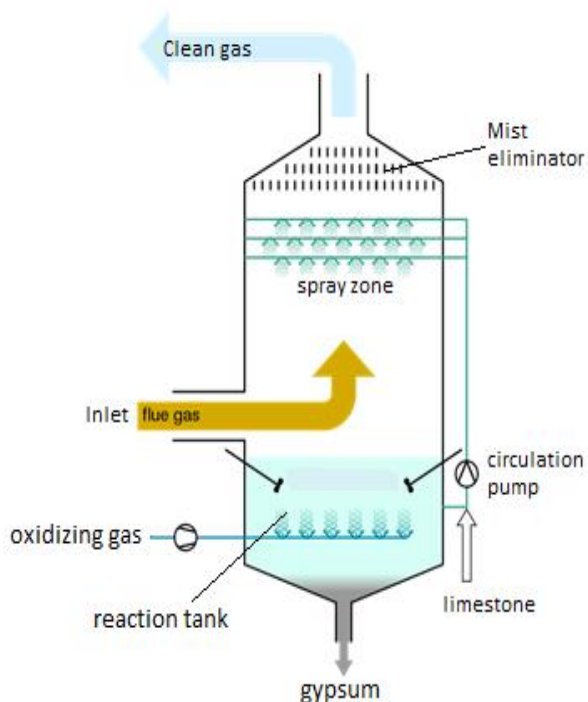
Absorber Unit Operations:

- Inlet – *gas distribution*
- Spray zone – *gas/liquid contact*
- Mist eliminator – *liquid/gas separation*
- Reaction tank – *oxidation, dissolution, crystallization*

Design Goals

- Lowest lifecycle cost
  - *capital*
  - *operating and maintenance*
- High reliability

Figure 3 - Open spray tower absorber [5]

1.4 Aim of the thesis and objectives.

The aim of this work is related to environmental protection technologies and the methods of reducing gaseous pollutants, such as SO_2, emitted into the atmosphere by coal power plants. Burning coal for electricity production is still a major concern which every country has to deal with. In order to minimize the adverse effects of SO_2 emission into the environment, power plants and industrial facilities use different methods of flue-gas desulfurization scrubbers to remove SO_2 from flue-gas. The research activities in this area are extensive, mainly because of the environmental protection policies regarding the emission of harmful pollutants.

This work deals with the method of Wet Flue-Gas Desulfurization (WFGD), in which, limestone suspension, is used to have chemical reaction with SO_2 molecules from flue-gas.

First objective of this work was to create a three-dimensional CFD model of the scrubber. For our model we considered to use a simplified, reduced-scale scrubber for the reason of faster evaluation of data. The second objective of the work was to simulate the flow of flue-gas passing through the scrubber. The mixture of components for the flue-gas in this work was considered only between air and sulfur dioxide. The third objective was to investigate the flow, in which the particles of limestone suspension were added into the scrubber by spray nozzle located inside of it, and lastly, investigate the chemical reactions between SO_2 and limestone suspension.

The data of flue-gas and limestone suspension were obtained from mainly three articles dealing with wet flue-gas desulfurization process, [1], [7], [8].

Once the data for flue-gas and limestone suspension were introduced into the software and run the simulations, different quantities (velocity profiles, concentration of mixture, concentration of suspension, turbulent kinetic energy and dissipation rate) were compared between the continuous phase and dispersed phase flow. For concentration of particles of limestone suspension, four different domain discretization have been simulated, with very coarse, coarse, medium, and fine grid, and the results were analyzed and compared between each other.

Chapter 2: Theory of wet flue-gas desulfurization

2.1 Chemistry fundamentals for reaction of limestone with SO₂

As described from the objectives, this work is focused in the wet limestone scrubbing method. In wet limestone scrubbing systems, a complex series of kinetic and equilibrium controlled reactions occur in the gas, liquid and solid phases [7].

This reactions can be divided in mainly five different steps, all of which occur simultaneously in the scrubber. The steps are: absorption, neutralization, regeneration, oxidation and precipitation [7]. For this work the chemical model is concentrated only in the reactions occurring in the spray zone, where the gas-liquid flow is analyzed. Therefore, regeneration, oxidation and precipitation processes are not considered further here because they mainly occur in the reaction tank, as illustrated in Figure 4.

1) Absorption – *(Spray zone)*

$$SO_{2,aq} + H_2O \rightleftarrows HSO_3^- + H^+$$
$$HSO_3^- \rightleftarrows SO_3^{2-} + H^+$$
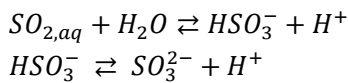
2) Neutralization – *(Spray zone)*

$$CO_3^{2-} + H^+ \rightleftarrows HCO_3^-$$
$$HCO_3^- + H^+ \rightleftarrows CO_{2,aq} + H_2O$$
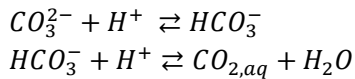
3) Regeneration – *(Reaction tank)*

$$CaCO_{3(s)} \rightleftarrows Ca^{2+} + CO_3^{2-}$$

4) Oxidation – *(Reaction tank)*

$$HSO_3^- + \frac{1}{2}O_2 \rightleftarrows SO_4^{2-} + H^+$$
$$SO_3^{2-} + \frac{1}{2}O_2 \rightleftarrows SO_4^{2-}$$
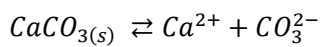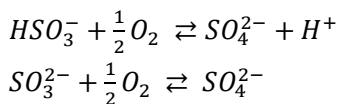
5) Precipitation – *(Reaction tank)*

$$Ca^{2+}SO_4^{2-} + 2H_2O \rightleftarrows CaSO_4 \cdot 2H_2O$$
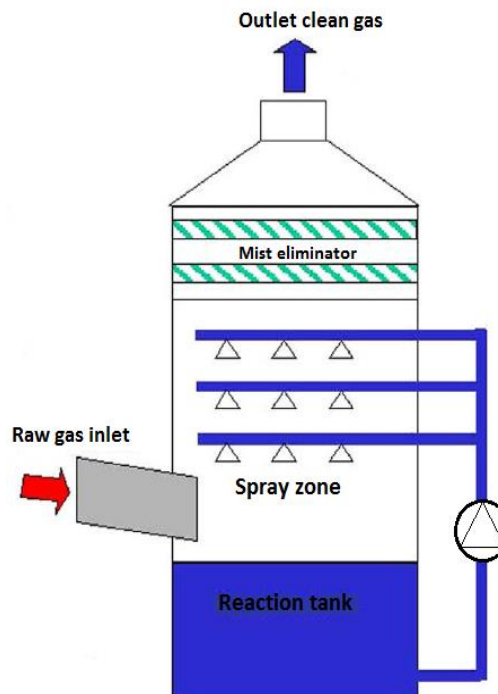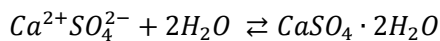
Figure 4 - Schematic picture of a WFGD scrubber along with the chemical reactions occurring inside of it, **[7]**

Critical aspects of operation include ensuring proper SO₂ removal at all times, maximizing reagent utilization and minimizing scale build-up on scrubber components.

The process of SO₂ removal from flue-gas, is a classic example of an aqueous acid-base chemistry reaction applied on an industrial scale, where alkaline limestone slurry reacts with acidic SO₂.

The slurry absorbs the SO_2 from the flue gas and the calcium in the limestone reacts with the SO_2 to form a mixture of calcium sulfite and calcium sulfate. The reaction system is very complex and many different processes take place inside the absorber and in the reaction vessel.

Sulphur dioxide is first absorbed into the liquid phase as it contacts the slurry sprays.

$$SO_2 + H_2O \Leftrightarrow H_2SO_3$$
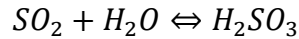
Some theoretical chemists argue that true H_2SO_3 does not exist and that SO_2 retains its molecular character and is surrounded by water molecules. However, when SO_2 is added to water the pH drops, which suggests this equation is reasonable and that the following dissociation reaction is accurate [2],

$$H_2SO_3 \Leftrightarrow H^+ + HSO_3^- \Leftrightarrow H^+ + SO_3^{2-}$$

Another argument for the formation of H_2SO_3, and its dissociated products bisulfite (HSO_3) and sulfite (SO_3^{2-}) ions, comes from the fact that the principal component of limestone, calcium carbonate ($CaCO_3$), is only slightly soluble in water but will dissolve almost completely in well-designed scrubbing systems [2],

$$CaCO_3 + H^+ \longrightarrow Ca^{2+} + HCO_3^-$$
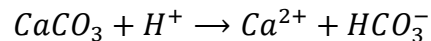
Combining these three equations illustrates the simplified but fundamental wet-limestone scrubbing process.

$$CaCO_3 + 2H^+ + SO_3{}^{2-} \longrightarrow Ca^{2+} + SO_3{}^{2-} + H_2O + CO_2$$
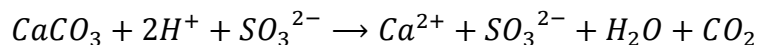
In the absence of any other reactants, calcium and sulfite ions will precipitate as a hemihydrate, where water is actually included in the crystal lattice of the scrubber byproduct.

$$Ca^{2+} + SO_3^{2-} + \frac{1}{2}H_2O \longrightarrow CaSO_3 \cdot \frac{1}{2}H_2O$$
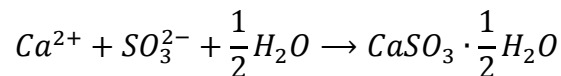
Proper operation of a scrubber is dependent upon the efficiency of the above-listed reactions. Control of pH via reagent feed is very important. Many wet-limestone scrubbers operate at a solution pH of around 5.2 to 5.8. A too-acidic scrubbing solution inhibits SO_2 transfer from gas to liquid; while an excessively basic slurry (pH > 6.0) indicates overfeed of limestone.

Oxygen in the flue gas greatly influences chemistry. Aqueous bisulfite and sulfite ions react with oxygen to produce sulfate ions (SO_4^{2-}) [2],

$$2SO_3^{2-} + O_2 \rightarrow 2SO_4^{2-}$$
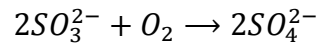
Approximately the first 15% mole of sulfate ions co-precipitates with sulfite to form calcium sulfite-sulfate hemihydrate [($0.85CaSO_3 \cdot 0.15CaSO_4$)·½$H_2O$]. Any sulfate above the 15 % mole ratio precipitates with calcium as gypsum [2],

$$Ca^{2+} + SO_4^{2-} + 2H_2O \rightarrow CaSO_4 \cdot 2H_2O$$
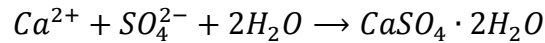
Control of by-product chemistry offers interesting challenges, particularly in spray towers that have internal devices to enhance gas-liquid contact. From Beychok [2], it is shown that operation in either a completely oxidized state (no calcium sulfite-sulfate hemihydrate in the scrubbing slurry) or a completely non-oxidized state (no gypsum in the slurry) minimizes scaling of internal scrubber components.

An often critical factor regarding the choice of oxidized or non-oxidized by-product involves the handling characteristics and commercial value of the solid. Calcium sulfite-sulfate hemihydrate is a soft material that tends to retain water. It has little value as a chemical commodity.

For this reason, many scrubbers are equipped with forced-air oxidation systems to introduce additional oxygen to the scrubber slurry. A properly designed oxidation system will convert all of the liquid sulfite ions to sulfate ions.

Sulfate, of course, precipitates with calcium as gypsum, which forms a cake-like material when subjected to vacuum filtration. Generally, 85 to 90 % of the free moisture in gypsum can be extracted by this relatively simple mechanical process. High-purity, dried synthetic gypsum has become a favorite material of wallboard manufacturers [9].

2.2 Critical scrubber design issues

An important concept regarding spray tower scrubbers is the liquid-to-gas (L/G) ratio. The proper amount of slurry must be present to allow SO_2 to pass from the gas phase to the liquid phase. The common unit of measurement for the L/G ratio is liters per minute of slurry to actual cubic meter per minute of flue-gas, where a baseline rule-of-thumb was once 15 l/m3. The L/G ratio is strongly influenced by the efficiency of liquid/gas mixing within spray towers [9].
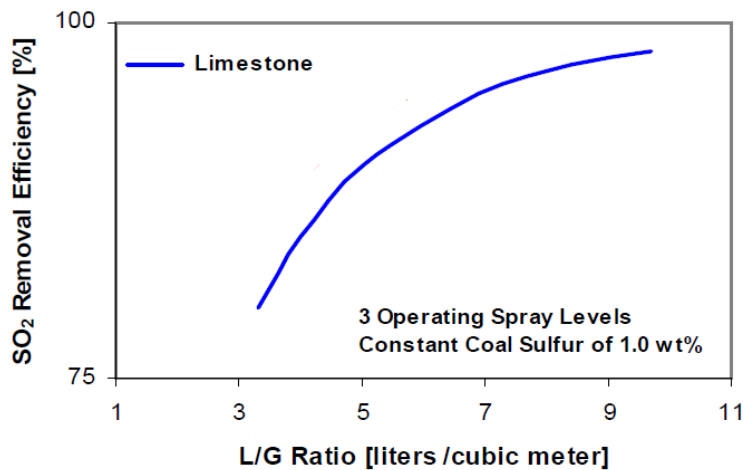
Figure 5 - SO_2 removal efficiency in function of L/G ratio **[5]**

Nozzle design and alignment are critical in these systems, as droplet size and spray patterns must be optimized to provide the best contact and to prevent channeling of the flue gas.

Limestone utilization in the scrubber is another important issue. If the limestone reacts poorly in the system, overfeed is required for adequate SO_2 removal. This of course results in excess reagent usage. Limestone costs for large scrubbers may reach or exceed a million dollars per year, so loss of reagent because of poor utilization can be rather expensive [9].

Factors that influence utilization include limestone quality, limestone grind size, residence time of the reagent within the scrubbing system and performance of slurry separation devices. Limestone reactivity is important with regard to scrubber operation. The chemical make-up of the reagent has a large influence on scrubber efficiency. Limestones containing 94 % or more $CaCO_3$ are very reactive, given of course that they are ground properly [9].

But not all plants are near high-quality limestone sources. Often, a stone may contain greater than 90 % total carbonate, but 10 % or more exists as dolomite ($MgCO_3 \cdot CaCO_3$), in which the magnesium is bonded with calcium in the crystal lattice. While pure $MgCO_3$ dissolves quickly in scrubber solutions, and provides liquid alkalinity, dolomite is rather non-reactive, and tends to pass through the system untouched. Utilities without access to high-purity limestone may need to enhance slurry reactivity with additives [9]

Regarding the desulfurization efficiency of wet scrubbers, the table 1 presented by Warych and Szymanowski [10], shows the relationship between different process parameters and desulfurization efficiency.

Parameter	Units	Range of parameter value	Min and Max efficiency value %
Slurry pH		5.2 – 5.8	86.4 – 93.5
Drop diameter	µm	2000-3000	74.5 – 99.3
Height of the absorber	m	6 – 18	66.5 – 99.7
Magnesium concentration	$kmol/m^3$	0.03 – 0.13	66.4 – 95.0
Chloride concentration	$kmol/m^3$	0.1 – 0.3	83.6 – 93.4
Inlet SO_2 concentration	ppm	1500 - 5000	73.4 – 97.0
Gas velocity	m/s	2 - 5	90.0 – 98.9
L/G ratio	l/m^3	8 - 15	68.3 – 97.7

Table 1 – Relationship between process parameter and desulfurization efficiency

2.3 Multiphase Model for CFD simulations

The major concern when dealing with multiphase flow in CFD is, which model is suitable to use for the particular multiphase problem. Now, depending on what type of flow regime exist in the investigated problem, the following table shows the relationship between the types of flow regimes to CFD multiphase models available in Ansys Fluent software.

Type of Flow	Eulerian model	Mixture model	VOF	DPM
Bubbly, droplet, and particle-laden flows Volume fraction $\leq$ to 10 %				✓
Bubbly, droplet, and particle-laden flows in which the phases mix and/or dispersed-phase volume fraction exceed 10%	✓	✓		
Slug flows			✓	
Stratified/free surface flows			✓	
Fluidized Beds	✓			

Table 2 – Relationship between types of flow and CFD multiphase model (Ansys Fluent guide)

The first flow regime in the table is, bubbly, droplet and particle-laden flows in which the volume fraction is less than or equal to 10 %. For such a type of flow regime we usually prefer the Discrete Phase Model (DPM), because of the Eulerian-Lagrangian approach applicable. [11]

The second flow regime, bubbly, droplet and particle-laden flows is the same flow regime as the first one, but in this case the dispersed-phase volume fraction is more than 10 %. In such case we cannot use the Eulerian-Lagrangian approach and hence we have to use Eulerian approach. For such flows also the Mixture Model is applicable.

The third flow regime is slug flow, for which the VOF model is applicable, because we have a distinct or separate phase we can interface between them.

The next type is stratified/free surface flows. As we have a free surface as a distinct interface between two phases we use again Volume of Fluid Model (VOF), and in case we are modeling fluidized beds we generally use the Eulerian Model [11].

Apart from the above flow regimes, there are also various other guidelines based on some terminologies or some basic physics. These terminologies are defined from particulate loading term. Particulate loading is defined as the mass density ratio of dispersed phase to that of the carrier phase. It gives as an indication of how the coupling is between the dispersed phase and the carrier phase, i.e. whether the dispersed phase also affects the flow of the carrier phase (continuous phase), is this coupling one-way or two-way etc.

Types of Flow	Flow physics	Multiphase Model
Very low loading	The coupling between the phases in one-way	Discrete phases, mixture, and Eulerian
Intermediate loading	The coupling is two-way	Discrete phases, mixture, and Eulerian models
For high loading	Two-way coupling plus particle pressure and viscous stresses due to particles (four-way coupling)	Only the Eulerian model

Table 3 – Coupling between phases in different types of flow

Based on table 3, there are three categories of flow: Very low loading of the dispersed phase and the particulate loading number is very low. In such cases the coupling between the phases is one-way, i.e. only the continuous phase is affecting the dispersed phase. Dispersed phase is not affecting the flow of the continuous phase. For these cases we can use the Discrete Phase Model, the Mixture model or the Eulerian model. When we have intermediate loading in which the particulate loading number is average, in such cases the coupling is two-way, i.e. the continuous phase is affecting the dispersed phase as well as due to motion of the dispersed phase the flow of the continuous phase is also disturbed. For these cases we use the Discrete Phase Model, Mixture model and Eulerian model. For high particulate loading in addition to two-way coupling there is

also particle pressure and viscous stresses due to particles, hence it is ranged as a four-way coupling. For these cases we use only the Eulerian model [11].

2.3.1   Eulerian – Lagrangian – steady state simulations (coupled)

"Coupled" it means we solve the continuous phase equations and dispersed phase equations together and simultaneously. For steady state simulations we have a steady state solution and hence we do not need to calculate at each time step, we will just calculate the steady state solution. So for this reason, we only solve Eulerian steady state equations for continuous phase flow – "steady state" means there will be no transient term, there is no differential with respect to time in the governing equations. Once we have solved steady state equations for the continuous phase, we solve Lagrangian equation of motion for dispersed phase and we track them from inlet to outlet, i.e. we solve the entire trajectory of the dispersed phase, i.e. the entire steady state trajectory. Once we have obtained the trajectory and the velocity for the dispersed phase the next step is to calculate the mass, momentum and energy source term. We obtain this and put them back in the governing equation for the continuous phase. We continue this process till we get a steady solution that is a non-changing solution for the trajectories as well as the velocity field of the continuous phase. So, our steady state convergence, will be a stable steady state continuous phase flow field and the steady state trajectory and flow field for the dispersed phase [11].

2.3.2   Eulerian – Lagrangian – Transient simulations (coupled)

There are basically four steps in this particular algorithm. The first step is to solve the transient governing equations for continuous phase flow at each cell volume, then at the end of each continuous phase time step calculate the dispersed phase velocities and trajectories using the Newton's law of motion. Then, based on these velocities and trajectories calculate the exchange source terms for mass, momentum and energy for that particular time step. Next is to put these mass, momentum and energy source terms into the governing equations for the continuous phase and then for the next time step again solve the continuous phase governing equations using the source terms calculated for the earlier time step. We will repeat this procedure till we get a converged solution for each time step and progress in time [11].

2.4 Mathematical models of mass transfer for WFGD process

In view of shortening development cycles and reducing development cost of wet scrubbers, it is very important to assess the performances of different setups and to confirm the influences of different design parameters in the early stages [8].

For this reason, the use of numerical simulation is a key factor. In the past two decades, significant progress has been made in the mathematical model of the wet flue gas desulfurization (WFGD) based on computational fluid dynamics (CFD) [12]. Comparing with the standard $k - \varepsilon$ turbulence model which is not suitable for flow with high mean shear rate or material separation, the Realizable $k - \varepsilon$ turbulence model is more appropriate for anisotropic turbulence and has been increasingly concerned in the studies of flow characteristics of the desulfurization towers [7]. Therefore, Marocco and Inzoli (2009), chose the realizable $k - \varepsilon$ turbulence model in their simulation studies and the simulation results were consistent with the experimental results very well.

The fluid dynamics inside an OST can be described as a gas-liquid two-phase flow consisting of a carrier gas and a large number of dispersed liquid droplets and can be modeled with Euler-Lagrange approach.

The Eulerian-Lagrangian model, involves less empirical equations and is more suitable for providing detailed information of the discrete phase. Furthermore, the heat transfer between gas and liquid phase can be also taken into account [7]. Hence, generally, the fluid dynamics of gas-liquid phase is modeled with the Eulerian-Lagrangian approach for volume fraction of discrete phase less than 10% [13].

In the Eulerian-Lagrangian approach, the continuous phase is modeled in Eulerian framework, while the discrete phase is modeled with Lagrangian approach by tracking the particles through the computational domain [14].

Compared with experimental method, numerical simulation method is more convenient, less costly and easier to evaluate the overall performance of the device [14]. Therefore, the two-phase flow was studied in this work by the CFD software package (Ansys-Fluent 16.2). The simulation for this work are conducted to a simplified scrubber. The simulations focuses mainly on the influence of the limestone slurry to the flow field of flue gas.

2.5 Governing equations in CFD

2.5.1 Carrier phase

The numerical model is based on the control volume method, which is standard in most of the commercial CFD codes. The continuous phase of particle-laden turbulent flow is traditionally approached using the Reynolds-Averaged Navier-Stokes (RANS) equations for mass, momentum and energy conservation [4].

The flue gas motion in the spray tower is modeled with the Eulerian approach. The liquid volume fraction, α_d, inside the scrubber is typically lower than 8-10 % everywhere, except very close to the spray nozzles. Because this region of high liquid volume fraction is limited to a small portion of the computational domain the following fundamental assumptions are justified:

a) The dispersed liquid phase occupies a low volume fraction and its effects on the continuous phase are negligible, i.e. $\alpha_d \to 0$ or $\alpha_c \to 1$, where α_d and α_c represents the liquid phase and the gas phase volume fraction, respectively.

b) The dispersed phase is sufficiently dilute so that interactions between particles are negligible.

c) The dispersed liquid phase consists of spherical droplets.

Considering the assumptions above, the conversation equations of the continuous phase assume then the same formulation as the conservation equations of a single phase flow with the addition of source terms, which represent mass, (S_{mass}) and ($S_{A,nass}$), momentum, (S_{mom}), and energy, (S_{en}), coupling between the phases: taken from work of L. Marocco and F. Inzoli [7].

$$\frac{\partial}{\partial t}\rho + \nabla \cdot (\rho \boldsymbol{u}) = S_{mass} \tag{1}$$

$$\frac{\partial}{\partial t}(\rho \boldsymbol{u}) + \nabla \cdot (\rho \boldsymbol{u} \otimes \boldsymbol{u}) = -\nabla p + \nabla \cdot (\tau + \tau^R) + \rho \boldsymbol{g} + S_{mom} \tag{2}$$

$$\frac{\partial}{\partial t}(\rho i) + \nabla \cdot (\rho \boldsymbol{u} i) = -p \nabla \cdot \boldsymbol{u} + \nabla \cdot (k_c \nabla T) + \rho \boldsymbol{u} \boldsymbol{g} + S_{en} \tag{3}$$

$$\frac{\partial}{\partial t}(\rho \omega_A) + \nabla \cdot (\rho \omega_A \boldsymbol{u}) = \nabla \cdot (\rho D_{AB} \nabla_{\omega A}) + S_{A,mass} \tag{4}$$

The above equations are valid for spherical, non-rotating droplets: ρ is the flue gas density, p the flue gas pressure, $\boldsymbol{g}$ acceleration of gravity vector, $\boldsymbol{u}$ and $\boldsymbol{v}$ the flue gas and droplet velocity vector, respectively, T the flue gas temperature, τ and τ^R are the shear stress and Reynolds stress tensor, respectively, i is the internal energy per unit mass, ω_A is the mass fraction of component A, D_{AB} is the binary diffusion coefficient of species A and B and k_c is the continuous phase thermal conductivity [7].

Turbulence energy and dissipation rate can be affected by the presence of dispersed particles. This effect is known as *turbulence modulation.* Source terms should be added in the equations of k and ε to account for turbulence modulation. Anyway, there is experimental evidence that modulation is weak if the particle concentration is very low, i.e.if $\alpha_d \to 0$. Therefore, the $k - \varepsilon$ realizable model has been used in its formulation for single-phase flows [15] [7].

The source terms S_{mass}, S_{mom}, S_{en}, and $S_{A,mass}$ are calculated by volume averaging the contributions from all the individual droplets within the cell volume [16].

$$S_{mass} = -\frac{1}{V}\sum_k \dot{m}_k \tag{5}$$

$$S_{mom} = -\frac{1}{V}\sum_k \boldsymbol{v}_k \dot{m}_k - \frac{1}{V}\sum_{i,k} \boldsymbol{F}_{i,k} \tag{6}$$

$$S_{en} = -\frac{1}{V}\sum_{i,k} \boldsymbol{F}_{i,k}\boldsymbol{v}_k - \frac{1}{V}\sum_k \dot{m}_k h_{1v,A} + \frac{1}{V}\sum_k \dot{Q}_k \tag{7}$$

$$S_{A,mass} = -\frac{1}{V}\sum_k \dot{m}_{A,k} \tag{8}$$

where the subscript k refers to the kth droplet, $\boldsymbol{v}$ is the droplet's velocity vector, $F_{i,k}$ is the sum of the forces acting at the interface between the phases, $h_{1v,A}$ is the latent heat of vaporization of component A and $\dot{Q}_k$ is the convective heat transfer between phases.

The source term of equation (1) represents mass exchange between phases due to droplet evaporation. The source term in equation (2) represent momentum exchange between phases due

to droplets' evaporation. The source terms of equation (3) represent energy exchange due to droplet evaporation. The source term in equation (4) represents mass exchange of species A between the phases due to evaporation [7].

After evaluation of these source terms, the gas-phase conservations need to be solved again (two-way coupling). The resulting flow, temperature and concentration fields are then used to calculate up-dated source terms and so on until convergence [7].

2.5.2 Dispersed phase

Once the gas velocity field is known, the particles' trajectories can be computed. In this work, the volume ratio of liquid phase is less than 10%. So, the liquid phase is treated as discrete phase in the Lagrangian frame by defining the injection type, velocity, diameter and so on. The dispersed liquid phase is calculated by tracking a large number of particles, called parcels, through the computational domain. The equations of motion of a single parcel take the following form [7]:

$$\frac{d\boldsymbol{x}}{dt} = \boldsymbol{v} \tag{9}$$

$$\frac{dm_d}{dt} = S_{k,,mass} \tag{10}$$

$$m_d \frac{d\boldsymbol{v}}{dt} = S_{k,mom} + m_d \boldsymbol{g} \tag{11}$$

$$m_d c_d \frac{dT_d}{dt} = S_{k,en} \tag{12}$$

The subscript d indicates that the quantity is referred to a droplet and c is the droplet's specific heat. Starting from the injection condition specified for each nozzle, these ordinary differential equations are solved by stepwise integration over discrete time steps, using the continuous phase flow properties at the current droplet position.

2.5.3   Flue gas properties

The flue gas flowing into the scrubber is a mixture of many species but only two of them are considered in this work. . So, for this work the flue gas is considered as a Newtonian mixture of sulfur dioxide and inert air. The gas phase it obeys the perfect gas law.

The *flue gas density* and *heat capacity* are functions of the mixture's temperature and composition. The thermal conductivity and the viscosity are constant all through the computational domain [7].

2.5.4   Slurry properties

The slurry droplets are considered a suspension of water, with dissolved species inside, and solids. The density of a droplet can vary during the trajectory calculation due to evaporation. It is evaluated at every point in the domain by providing the solids mass fraction of 15 % and the slurry density. The droplet viscosity has been assumed to vary with temperature as if it were water. The specific heat of a slurry droplet, c_d, has been assumed constant and equal to the specific heat of water at droplet's injection temperature [7].
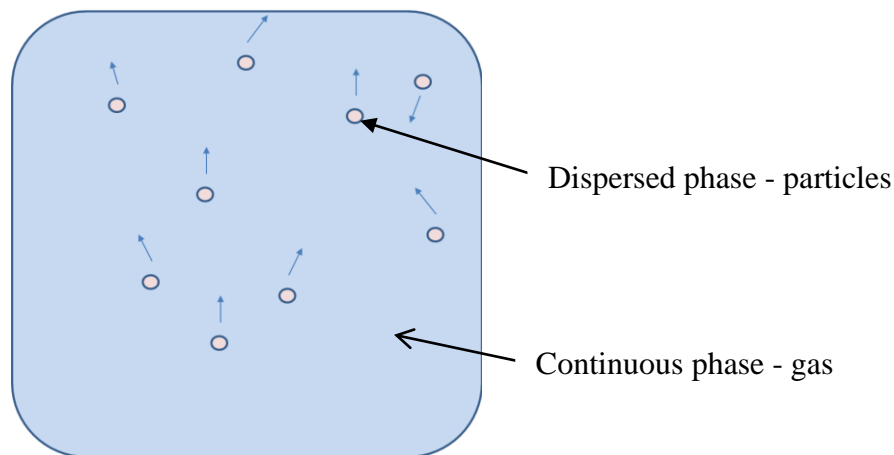
Figure 6 – Eulerian – Lagrangian approach illustration **[11]**

Chapter 3: Preparation and testing of numerical model

Since this work is focused in modeling the flow of flue gas with droplets of limestone slurry the geometry of the scrubber has been simplified in rectangular shape channel for purpose of conducting only the simulations regarding the flow and chemical reactions between the gas and liquid phase. Ansys Fluent 16.2 is used to predict the flow of flue gas (air + SO_2), and the behavior of the nozzle spraying the droplets of limestone.

The nozzle has not been geometrically modeled but it has been treated as an injection point. This simplification is justified by the negligible impact of the nozzle dimensions on the channel hydrodynamics compared to other geometrical entities. For this part Fluent software has the capability of inserting the spray nozzles as injections with taking the properties of nozzles and introducing them into the software.

To predict the behavior of spray nozzle, the discrete phase model (DPM) is used.

3.1   Problem description

The geometry to be considered in this work is shown in the Figure 8.

The flue gas enters at the bottom of the channel with velocity 5 m/s and flows upwards to the outlet. At the reaction zone (the part where limestone is injected, as seen from Figure 8) the flue-gas is contacted by the injected particles of limestone which tends to deform the streamlines of the gas directed through the outlet. The type of channel described in Figure 8 represents a simplified counter-current scrubber, with the geometry scaled for laboratory purposes with only one nozzle to be considered.

The injection point, which represents the nozzle, is located in coordinate 0, 0, 0.4 of the channel in height [m]. The reason for inserting only one spray injection is because of the small channel dimensions. The injection point will distribute enough suspension of limestone through the reaction domain.

The spray type is solid cone and angle of injection is 45°, which in Fluent software stands for the half angle of the cone, and the pattern of the spray looks like in Figure 7, which are shown also two other patterns of different types of spray nzzles for comparison.
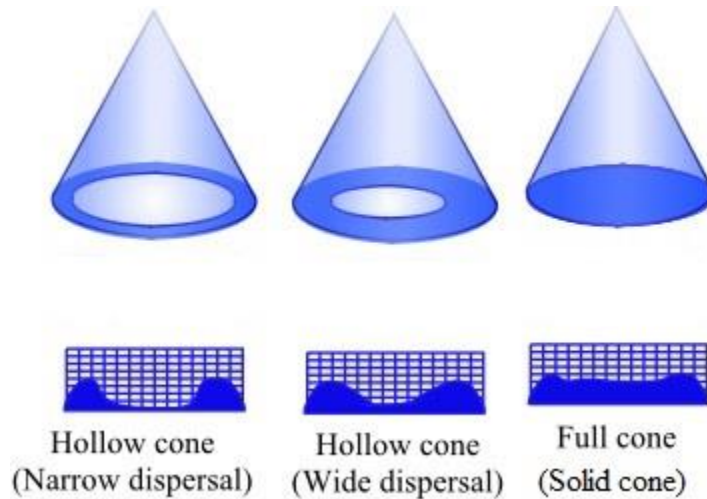
Figure 7 – Basic spray patterns

The data for flue-gas and limestone slurry are taken from three different articles dealing with wet flue-gas desulfurization process, [1], [7], [8].

The above equations described in paragraph (2.1) for the chemical reactions in terms of the reaction mechanism that happens into the channel, are complex and to be introduced into the software for each particle reaction requires correct evaluation of data. These data can be calculated based on values in chemical tables and chemical theory for reaction kinetics.

The chemical reactions intended to takes place in the channel and which will be considered in this work are categorized in two basic processes: mainly the physical absorption of the molecule of sulfur dioxide (SO_2), and the chemical reaction between sulfur dioxide (SO_2) and Calcium carbonate ($CaCO_3$).

The simulations to be performed in this work has this order;

1) Gas single-phase flow – Flue gas (air + sulfur dioxide)
2) Liquid-solid two-phase mixture – Limestone slurry
3) Gas-liquid two-phase flow - formed by adding 1st and 2nd phases together;

    1st + 2nd = gas-liquid phase (flue gas + limestone slurry).

The chemical reaction to be considered in this work is:

$$CaCO_3 + SO_2 \rightarrow CaSO_3 + CO_2$$
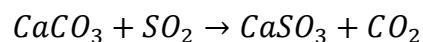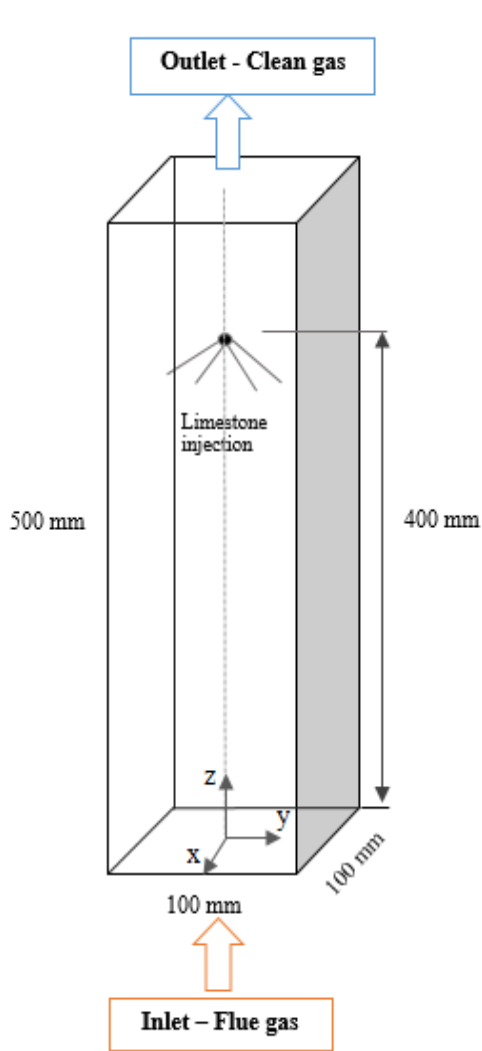
Channel configuration

Injection location (m)	[0, 0, 0.4]
Injection spray angle	45 °
Injection type	solid cone
Particles per injection 20	
Number of injections 1	

Boundary conditions

Flue gas data:

Density, ρ 0.84 kg/m3	
Dynamic viscosity, μ	$2 \cdot 10^{-5}$ N·s
Inlet gas velocity	5 m/s
Inlet gas temperature	100 °C
SO2 volume fraction, %	0.1

Liquid slurry data:

Slurry volume flow	0.02 kg/s
Slurry density	1103 kg/m3
pH	5.6
Slurry temperature	52 °C

Figure 8 - Main geometrical and simulation parameters of the continuous and discrete phase; data obtained by work of L. Marocco, K. Brown, Y.J. Xiao, [1], [7], [8].
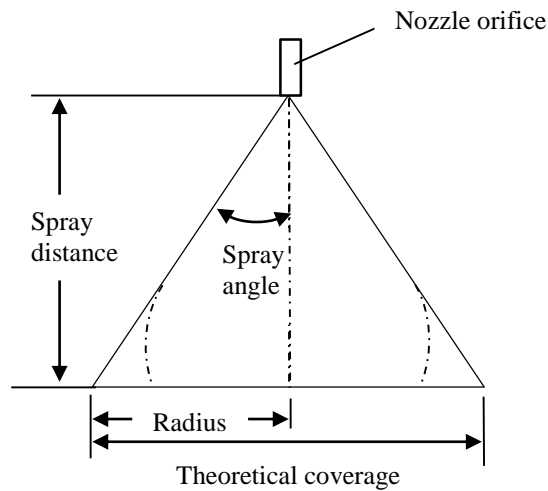
Figure 9 – Spray nozzle characteristics

3.2 Creation of geometry and mesh

The geometry of the channel consists of inlet, wall and outlet and was created in Ansys Workbench 16.2. The dimensions of the channel are as described in the Figure 8, with the inlet dimension of 01 x 01 m, and the height of the channel is 0.5m. To generate the mesh Ansys Fluent Mesher was used. Mesh consists of hexahedrons with the element size of 5mm and the number of elements is 39200. Size of mesh is in accordance with Courant-Friedrich-Lewy (CFL) theory conditions. Channel geometry and mesh are shown in Figure 10.

.

Zoom of a section cut
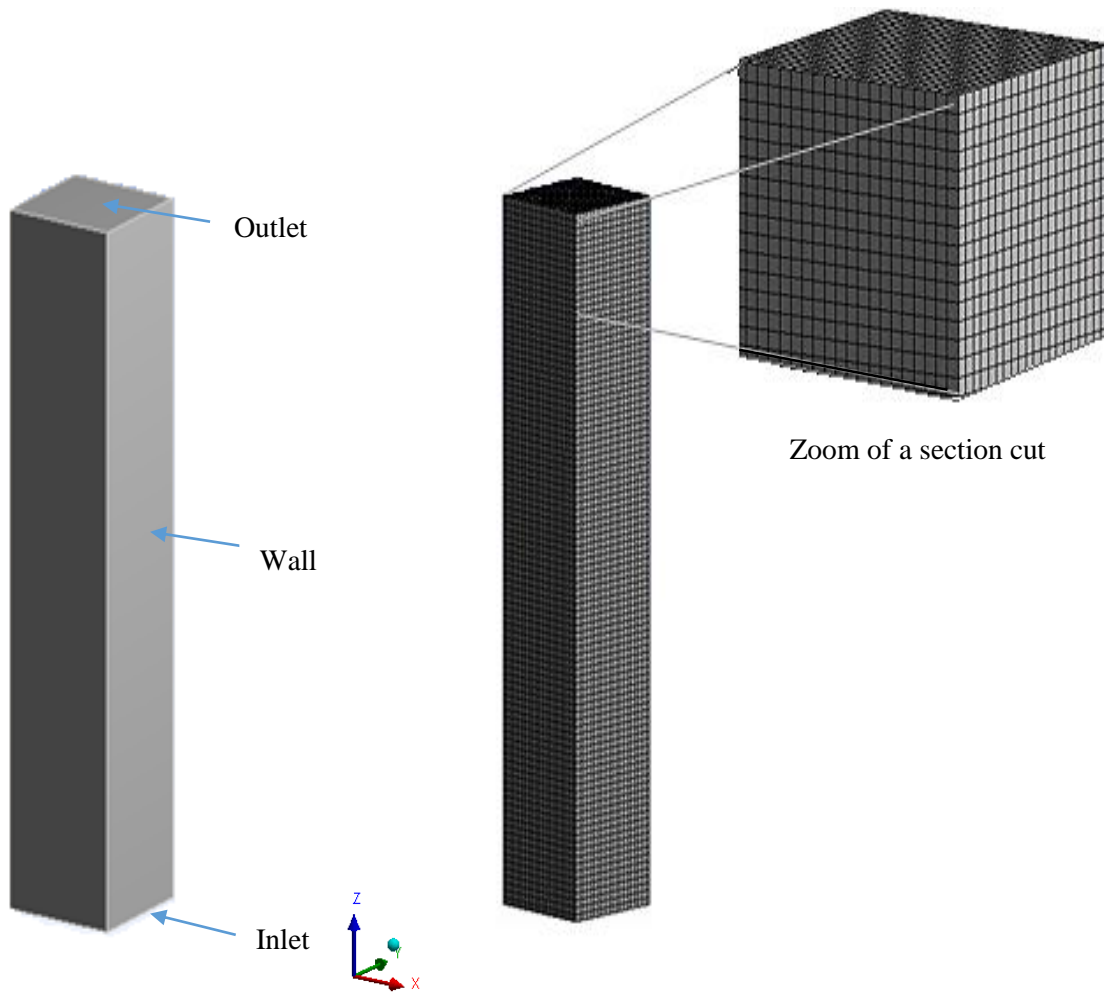
Figure 10 - Geometry and mesh of the channel

Physical interpretation of CFL theory conditions says: the distance travelled by the solution in one time step $c\Delta t$ must be less than the distance between two mesh points Δx.

$c\Delta t$ – solution in one time step

Δx – distance between two mesh points

1st order upwind CFL condition (for most explicit schemes) formula is:

$$\frac{c\Delta t}{\Delta x} \leq 1$$

So, for the velocity of the flow in the channel, $c = 5\,m/s$, and time step $\Delta t = 10^{-3}$, the element size Δx is found by the above formula;

$$\Delta x \geq c\Delta t$$

$$\Delta x \geq 5 \times 10^{-3}$$

The quality of the mesh is checked with Fluent mesh/check quality, and the report shows perfect accordance with the specified parameters for good quality mesh:

```
Mesh Quality:

Minimum Orthogonal Quality =  1.00000e+00
(Orthogonal Quality ranges from 0 to 1, where values close to 0 correspond to low quality.)

Maximum Ortho Skew =  2.91010e-07
(Ortho Skew ranges from 0 to 1, where values close to 1 correspond to low quality.)

Maximum Aspect Ratio =  1.74598e+00
```

To speed up the solution procedure, the mesh should be reordered, which will substantially reduce the bandwidth.

ANSYS Fluent will report the progress in the console:

Chapter 4: Numerical simulation of the wet scrubber

4.1 Simulation description

Within the computational region, CFD solves Navier-Stokes equations to obtain velocity, pressure, temperature and other quantities that may be required from problem description of the flow through the channel. The simulation consisted of inlet and outlet boundary conditions, set as, velocity inlet, and constant pressure outlet, respectively.

Air and sulfur dioxide inside the vertical channel were set as primary phase flow (Eulerian approach). The primary phase used models (momentum, turbulence and energy,) which uses boundary conditions as mentioned above in Figure 8.

The limestone injection was set as secondary phase (Lagrangian approach) where its inlet boundary conditions are based on spray injections parameters (determined empirically) as described in Figure 8. The Lagrangian particles were tracked using Discrete Phase Model (DPM). During computation, heat and mass transfer was coupled between primary and secondary phases.

The walls had a common (standard) setup, with no slip, adiabatic (insulated) and the heat flux from wall to fluid is zero.

The other important simulation data for the continuous phase and discrete phase are summarized in Figure 8.

4.2 General settings of the flue gas simulation

The pressure-based solver was used for the flow regime in the computational domain. The nature of the problem for the simulation - modeling the flow of flue-gas with droplets of limestone is transient in nature.

Another important parameter to be checked before continuing with other data input, is the gravitational acceleration, which needs to be set in right direction. This is done because the injected particles has to go downward of the channel, and for this reason the –z direction is applied for gravity.

The Eulerian multiphase model is enabled with two Eulerian phases which stands for; air + sulfur dioxide. The heat transfer between the phases is enabled by the energy equation.
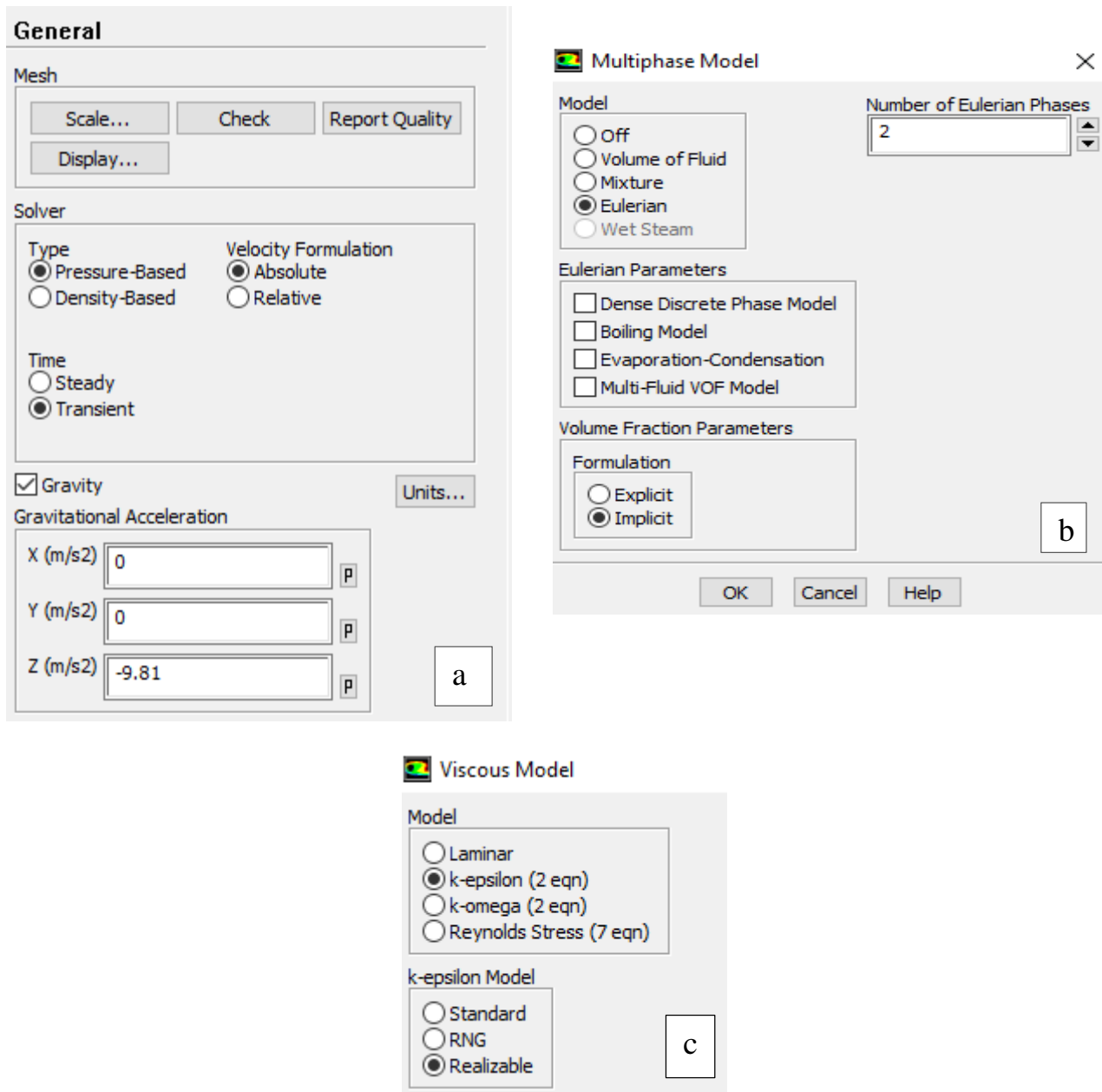
Figure 11 - General settings input; a) solver type, b) multiphase model, c) viscous model

The Realizable k-epsilon viscous model gives a more accurate prediction of the spreading rate of spray injection than the standard k-epsilon model, and for this reason it has been used for the simulation.

4.2.1   Setting up materials and boundary conditions

The inlet velocity magnitude of the flue gas is set to be 5 m/s. In the thermal tab for the temperature of flue gas in the inlet we set as 373 K. For the second component (SO_2), we use the same conditions, with attention in the multiphase volume fraction, which for SO_2 is 0.1 % in concentration. The pressure is retain as pressure outlet for both simulations. We initialize the solution without droplets.

The air + SO_2 flow will first be solved and analyzed without droplets of the discrete phase.

We enable the residual plotting during calculation.

We initialize the flow in hybrid method and we start the calculation by requesting 20 iterations for each time step, which for this case was set 1000 time steps and the time step size as calculated from the CFL method, is set to 0.001. Data files was saved for post-processing reason. We create clip planes aligned with surface of outlet and wall to examine the flow field at the midpoint of the channel and in the cut sections.

4.2.2   Scaled residuals of continuous phase
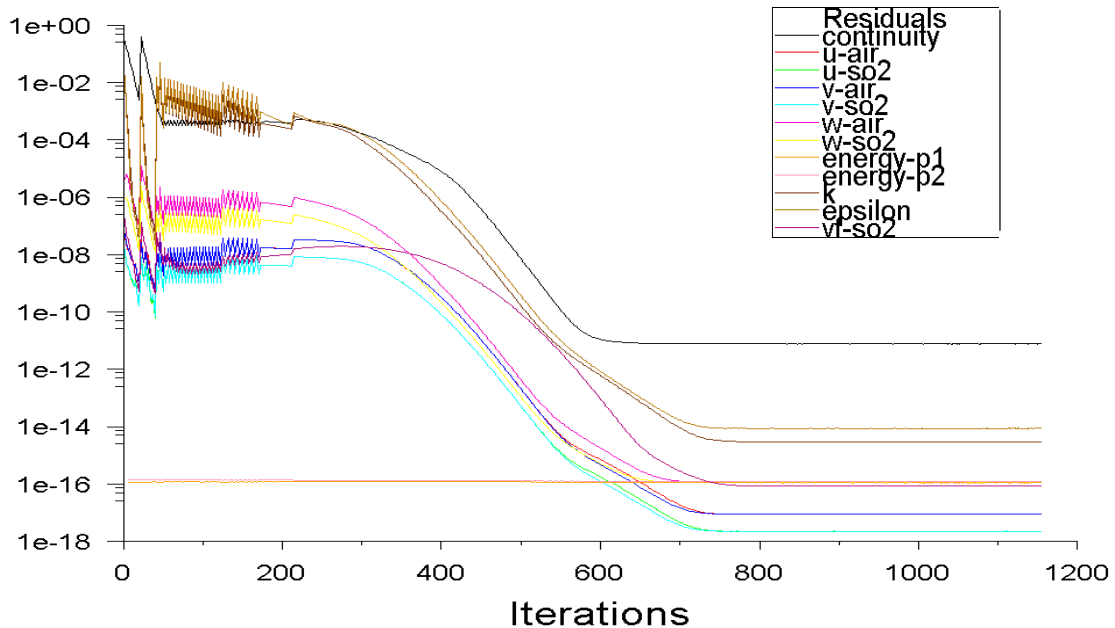
Figure 12 - Residuals of continuous phase

39

The residual criteria were set for different variables, which are; continuity, velocity, turbulent kinetic energy, volume fraction and energy. For energy the convergence criteria was set to 10^{-6}. The convergence of the solution was reached as seen from the fig.12 since this residuals were under the set criteria.

4.3 Results from continuous phase simulation
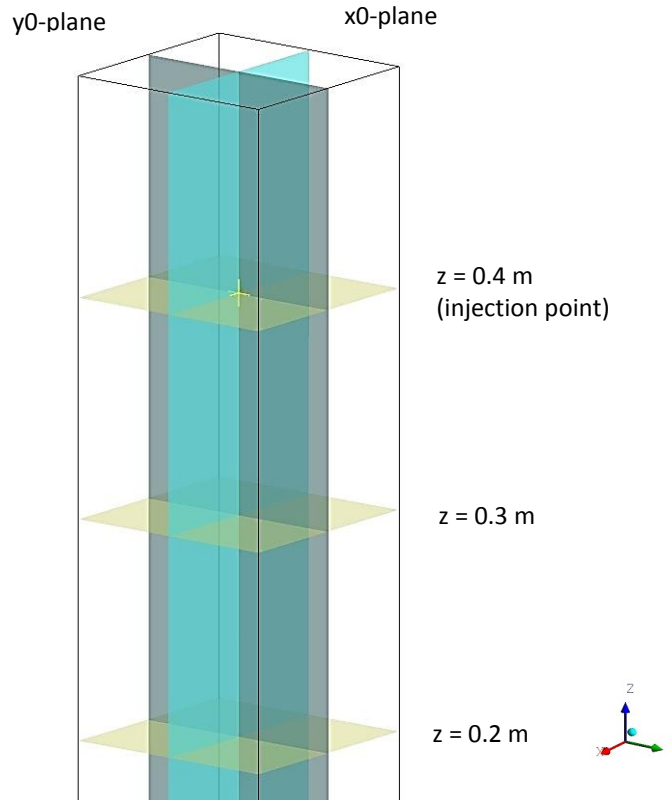
Figure 13 – Planes for displaying results

The created orthogonal planes for visualization of results was chosen in this arrangement for the purpose of investigating the symmetry of the flow through the channel. In the other hand, the planes aligned parallel to the outlet, z = 0.4m, z = 0.3m, and z = 0.2m, are created for the purpose of investigating the injection spray patterns.

For the continuous phase results, important quantities to be evaluated are, velocity profiles of air and SO_2, volume fraction of air and SO_2, and the turbulent kinetic energy of the mixture (air +SO_2).

*Velocity profiles for the continuous phase in **x0-plane***;
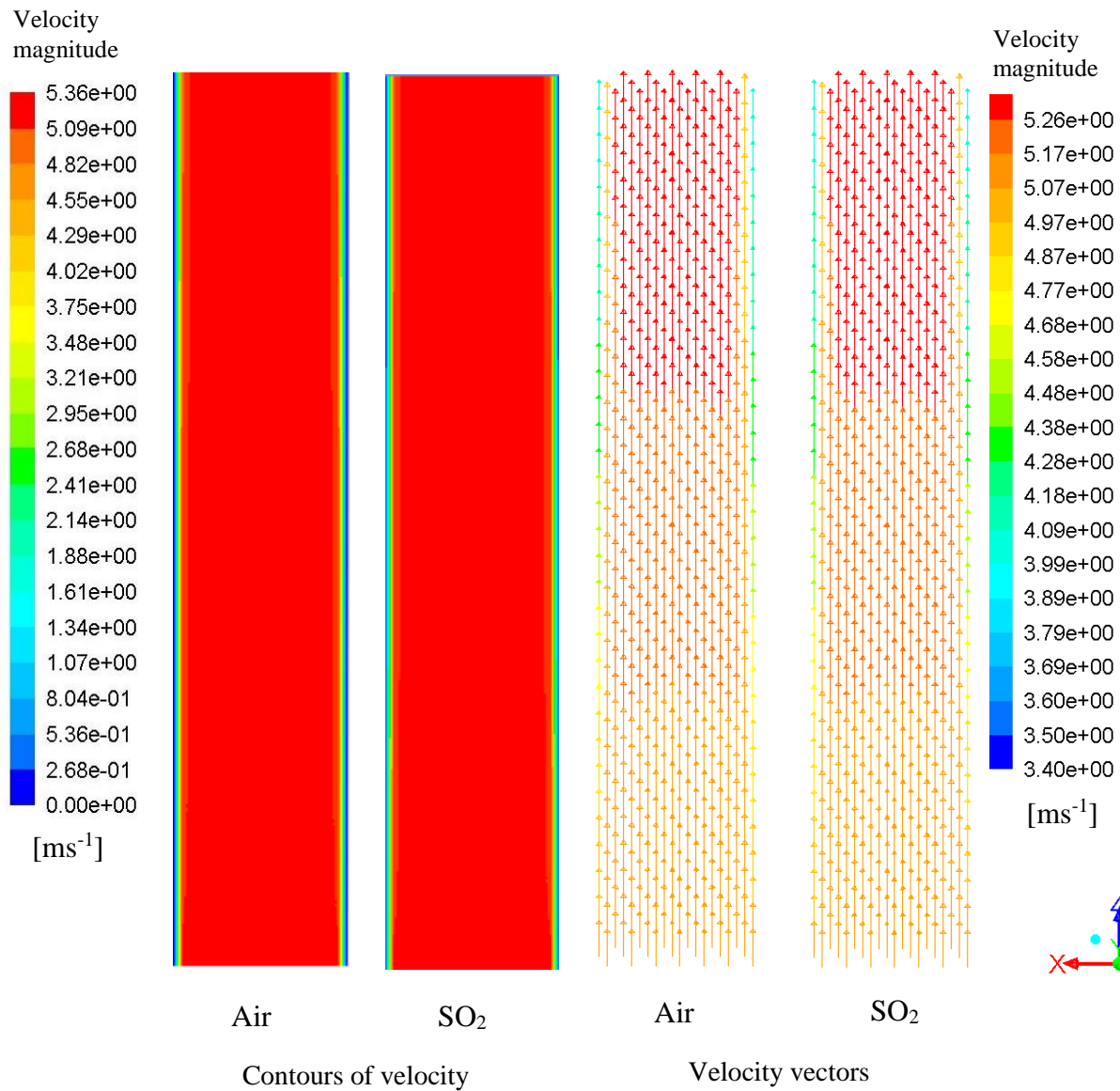
Figure 14 - Velocity profiles of continuous phase in x0-plane

In fig. 14 and fig.15, are shown contours and vectors of velocity magnitudes in two planes of the channel. Since the mixture of the gas consists of same initial velocity magnitude (5 m/s), the flow between separated components of the gas has no effect in each other.

*Velocity profiles for the continuous phase in **y0-plane**;*
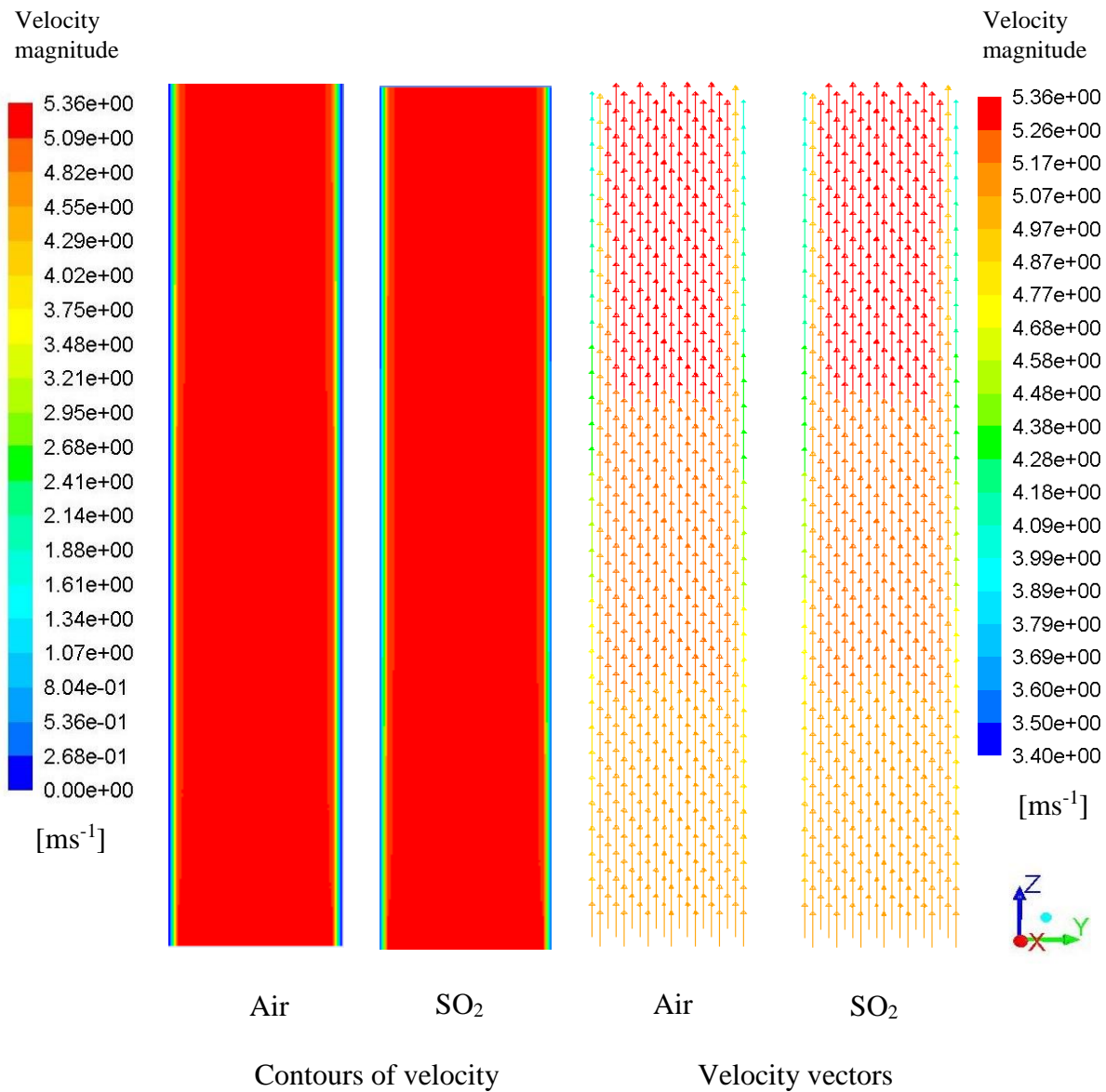
Figure 15 - Velocity profiles of continuous phase in y0-plane

From the fig. 14 and fig. 15, we can see that the velocity magnitude of the continuous phase (air + sulfur dioxide), it shows the symmetry of the flow. Because the symmetry in case of fluid flow calculations not depends only on geometrical symmetry, but the symmetry of all physical quantities, in this case, particle velocity of flue gas. The changes in velocity magnitude are seen near the walls of the channel which is caused by the friction forces between wall and gas.

Contours of volume fraction of air and SO₂ for the continuous phase;

Volume
fraction %

1.000e+000
9.286e-001
8.571e-001
7.857e-001
7.143e-001
6.429e-001
5.714e-001
5.000e-001
4.286e-001
3.571e-001
2.857e-001
2.143e-001
1.429e-001
7.143e-002
0.000e+000

Air
x0-plane

SO₂
x0-plane

Air
z = 0.4m

SO₂
z = 0.4m
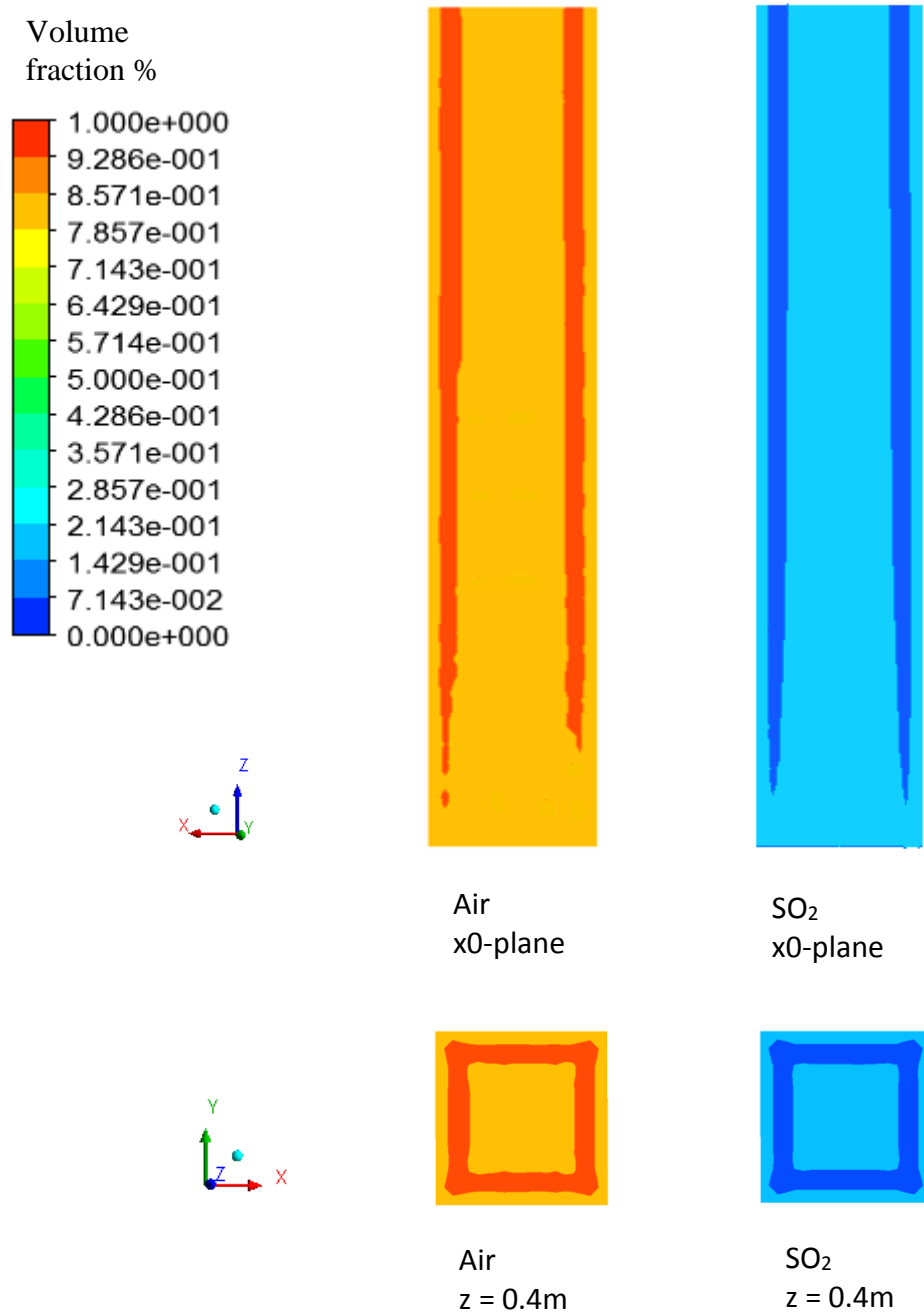
Figure 16 – Comparison between contours of volume fraction of air and SO₂ for continuous phase

From the fig.16 we can say that the model of mixture is working. Since everywhere in the channel we need to have 100 % of the mixture, from which 0.9 % air, and 0.1 % SO₂, so, from the

comparison of the concentration in x0 plane of the mixture, we can conclude that the parts with maximum volume fraction of air are in correlation with parts with minimum volume fraction of SO_2.

Turbulence kinetic energy and dissipation rate for the mixture (air +SO$_2$);

2.82e-01
2.64e-01
2.45e-01
2.27e-01
2.09e-01
1.91e-01
1.72e-01
1.54e-01
1.36e-01
1.17e-01
9.92e-02
8.10e-02
6.27e-02
4.44e-02
2.62e-02
7.91e-03

$[m^2/s^2]$

4.70e+01
4.38e+01
4.07e+01
3.76e+01
3.45e+01
3.13e+01
2.82e+01
2.51e+01
2.20e+01
1.89e+01
1.57e+01
1.26e+01
9.48e+00
6.35e+00
3.23e+00
1.03e-01

$[m^2/s^3]$

Turbulence kinetic energy   Turbulent dissipation rate

(air + SO$_2$)   (air + SO$_2$)
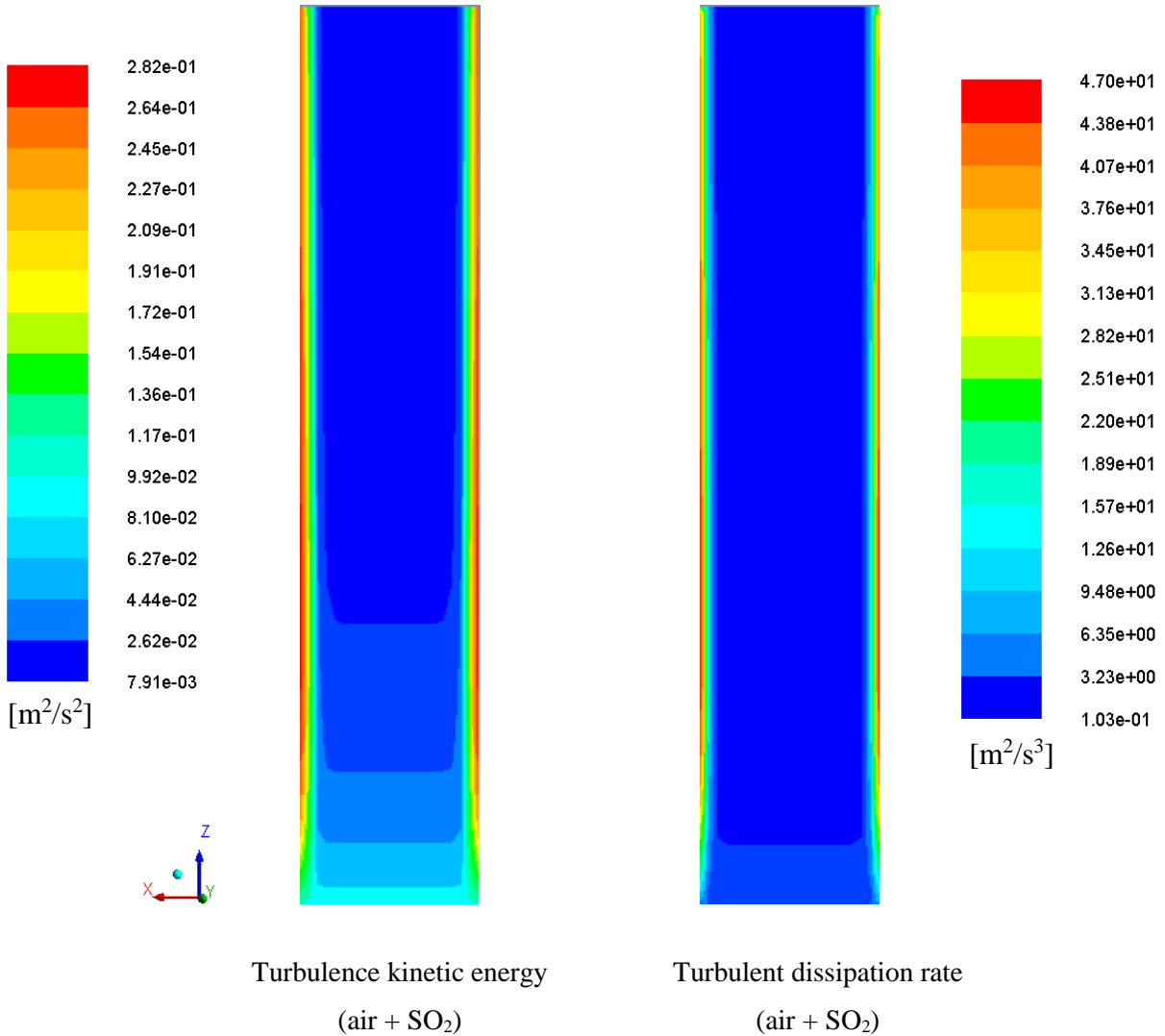
Figure 17 – Turbulence kinetic energy and dissipation rate of the mixture for continuous phase

The presented turbulent kinetic energy and dissipation rate is only shown for the mixture, since the Fluent model of turbulent energy cannot evaluate the results for each separate component of the mixture. In fact turbulent kinetic energy describes the type of flow, and from the figures

above we can see that the flow in the inlet is with small turbulences, and gradually changes to laminar by balancing between the uniform profile and the real profile of the flow.

4.4 Creating a spray injection

The spray injection for the limestone droplets is created by defining the discrete phase parameters. By selecting the interaction with continuous phase in the interaction group box, this will include the effects of the discrete phase trajectories on the continuous phase.

We retain the value of 10 for number of continuous phase iterations per DPM iteration.

By selecting the mean value in the contour plots for DMP variables, this will make the cell-averaged variables available for post-processing activities. We select the unsteady particle tracking in the particle treatment group box and we enter 0.001 for particle time step size. Also we enter 10 for the number of time steps.

Now we create the injection in the injection dialog box. In this step we will define the characteristics of the nozzle. We select solid cone for the injection type and we enter 100 for the number of particle streams. The particle stream option controls the number of droplet parcels that are introduced into the domain at every time step. Next steps to include in the injection are;

    a. We select inert in the particle type group box and select the calcium carbonate from the material drop-down list.

    b. In the point properties tab, we specify the point properties for particle injection.

    c. We enter 0.4 in the z position for the injection location. We retain the default values of 0, 0, and -1 for x axis, y axis, and z axis, respectively.

    d. For the temperature of the particles we enter 325 K.

    e. For the limestone flow rate we enter 0.02 kg/s.

    f. We retain the start time of 0s and enter 100s for the stop time. For this problem the injection should begin at t=0 and not stop until long after the time period of interest. A large value fort the stop time (for example, 100s) will ensure that the injection will essentially never stop.

    g. We enter 0.001 for the injection diameter (m) and 45 degrees for the cone angle (deg.).The spray angle is the angle between the liquid sheet trajectory and the injector centerline.

h. We enter 5 m/s for the relative velocity magnitude. The relative velocity magnitude is the expected relative velocity between of the injection slurry to the continuous phase.

i. Retain the default azimuthal start angle of 0 degrees and enter 360 degrees for the azimuthal stop angle. This will set the injection to spray in 360-degrees.

## *4.5   Results for discrete phase simulation*

For the discrete phase we evaluated the main physical quantities as for the continuous phase and the effect of the size and velocity distribution of the dispersed phase into the channel. This parameters are calculated by Fluent software after we input the injection data and run the calculations. To visualize the results two orthogonal planes, and three planes in z direction as described in Figure 13 were created.

The injection of inert particles of calcium carbonate into the channel have very small effect on the flow of continuous phase because of their small size in diameter. From this simulation can be evaluated different parameters of the discrete phase such as, distribution of the particles through the domain, trajectories of the particles, and the residence time of the particles in the channel.

Four different element size of the mesh, very coarse grid, 20 mm, coarse grid, 15 mm, medium grid, 10 mm, and fine grind, 5 mm, were simulated through the same initial input parameters for the discrete phase. The results of discrete phase concentration from the four simulations were compared between each other and an optimal element size for the mesh was estimated.

The charts of discrete phase concentration are shown in fig. 25 – 28, where the results were obtained by the report of surface integrals, with area weighted average for plane x0, y0 and planes in z direction which represents the height of the channel.

*Velocity profiles for the continuous phase in **x0-plane***;
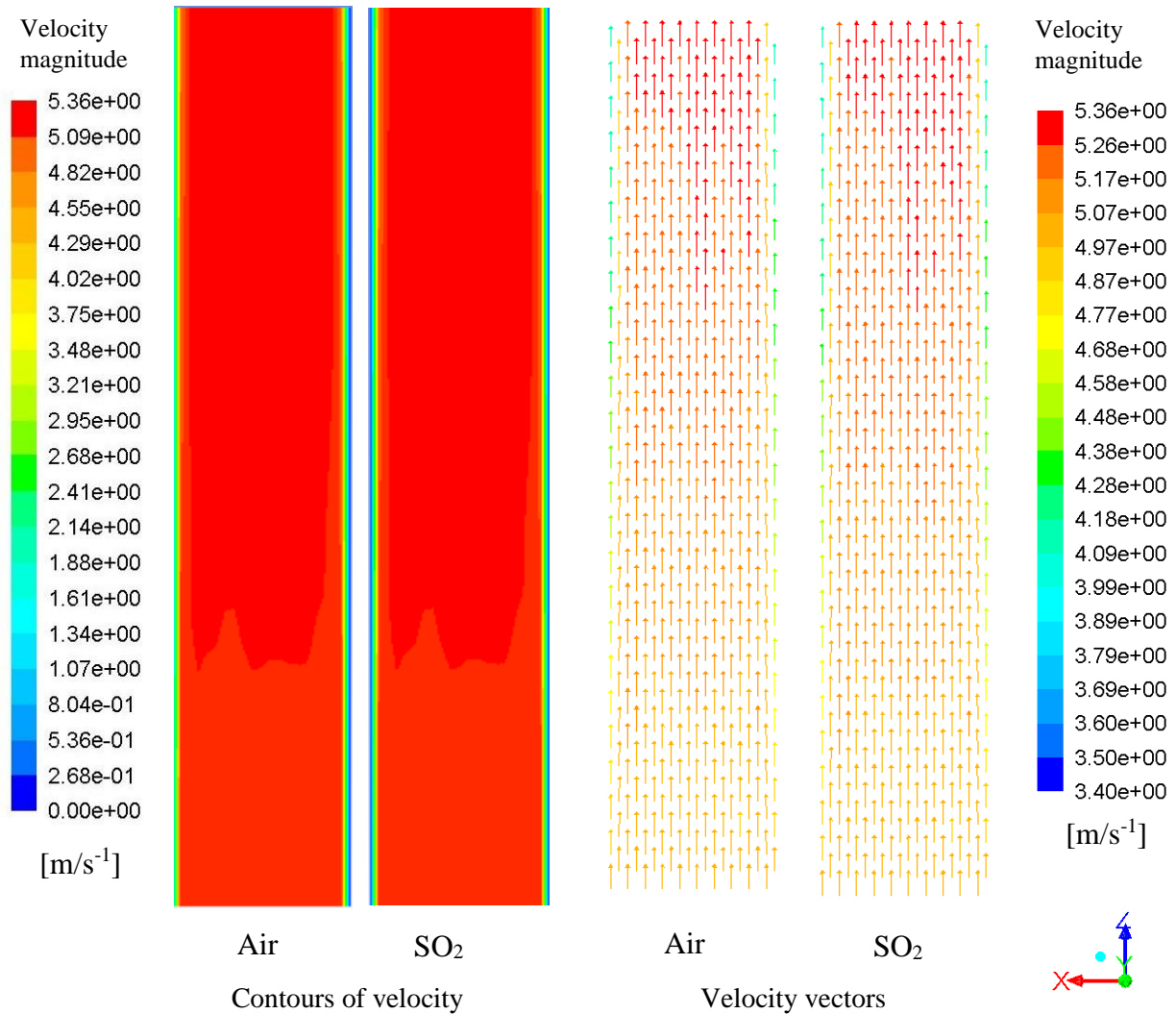
Figure 18 – Velocity profiles of continuous phase in x0 plane

The velocity profile for air and SO_2 is almost the same in the two planes since the geometry of the channel is uniform in shape. The only changing is near to the walls, and this is caused by the friction of the gas with walls of the channel. The inlet velocity is uniform through the inlet section.

*Velocity profiles for continuous phase in **y0-plane***;
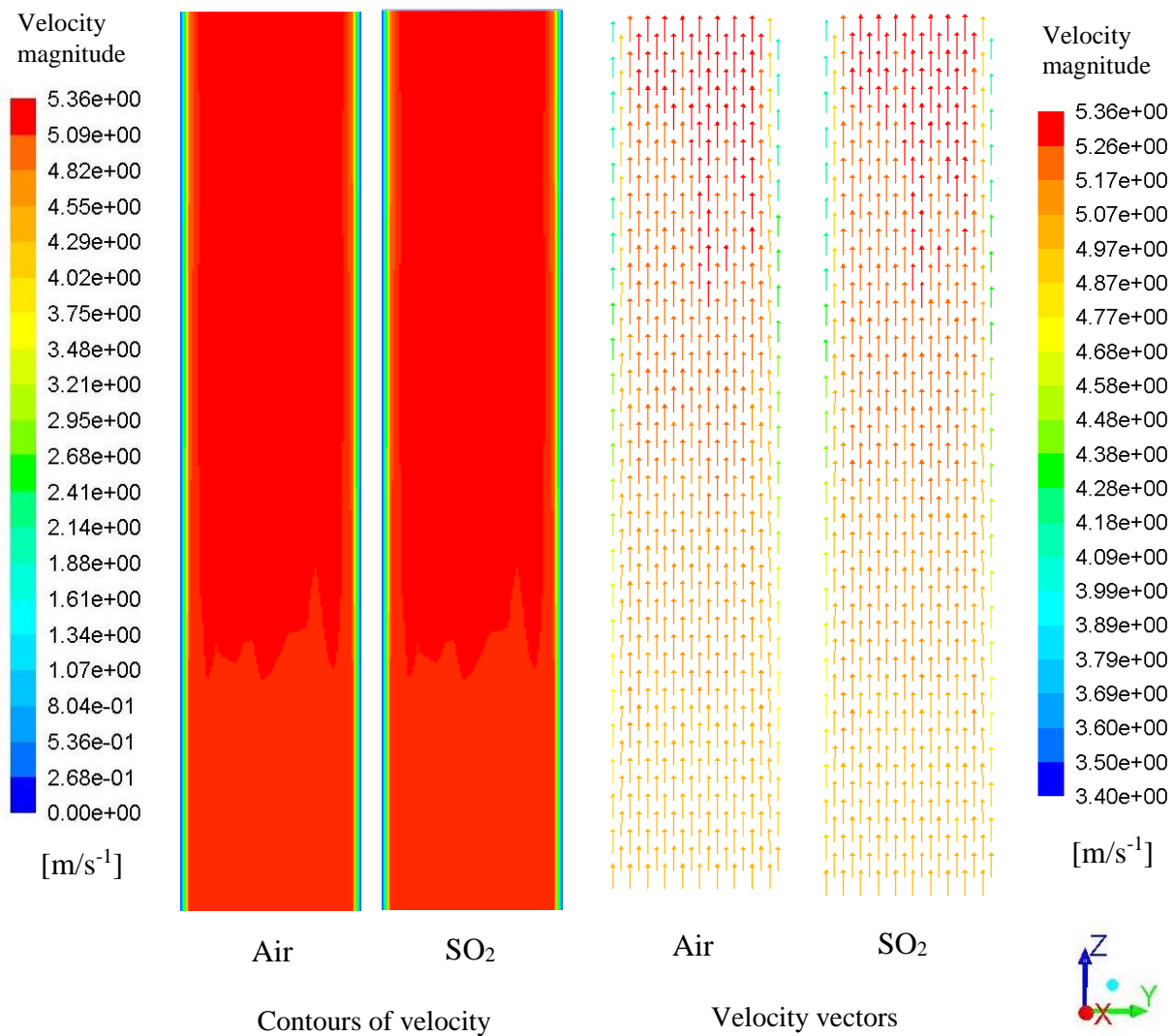
Figure 19 – Velocity profiles of continuous phase in y0 plane

If we compare velocity magnitude from continuous phase in Figure 14 and Figure 15, with velocity magnitude of continuous phase with discrete in Figure 18 and Figure 19, we see that the flow is quite similar, since the inert particles has very small effect in the flow of flue-gas and the symmetry of the flow still exist in both planes.

Contours of volume fraction of air and SO₂ ;

Air
x0-plane

Air
y0-plane

SO₂
x0-plane

SO₂
y0-plane

Air
z = 0.4m

Air
z = 0.3m

Air
z = 0.2m

SO₂
z = 0.2m

SO₂
z = 0.3m

SO₂
z = 0.4m

Figure 20 - Comparison between contours of volume fraction of air and SO₂
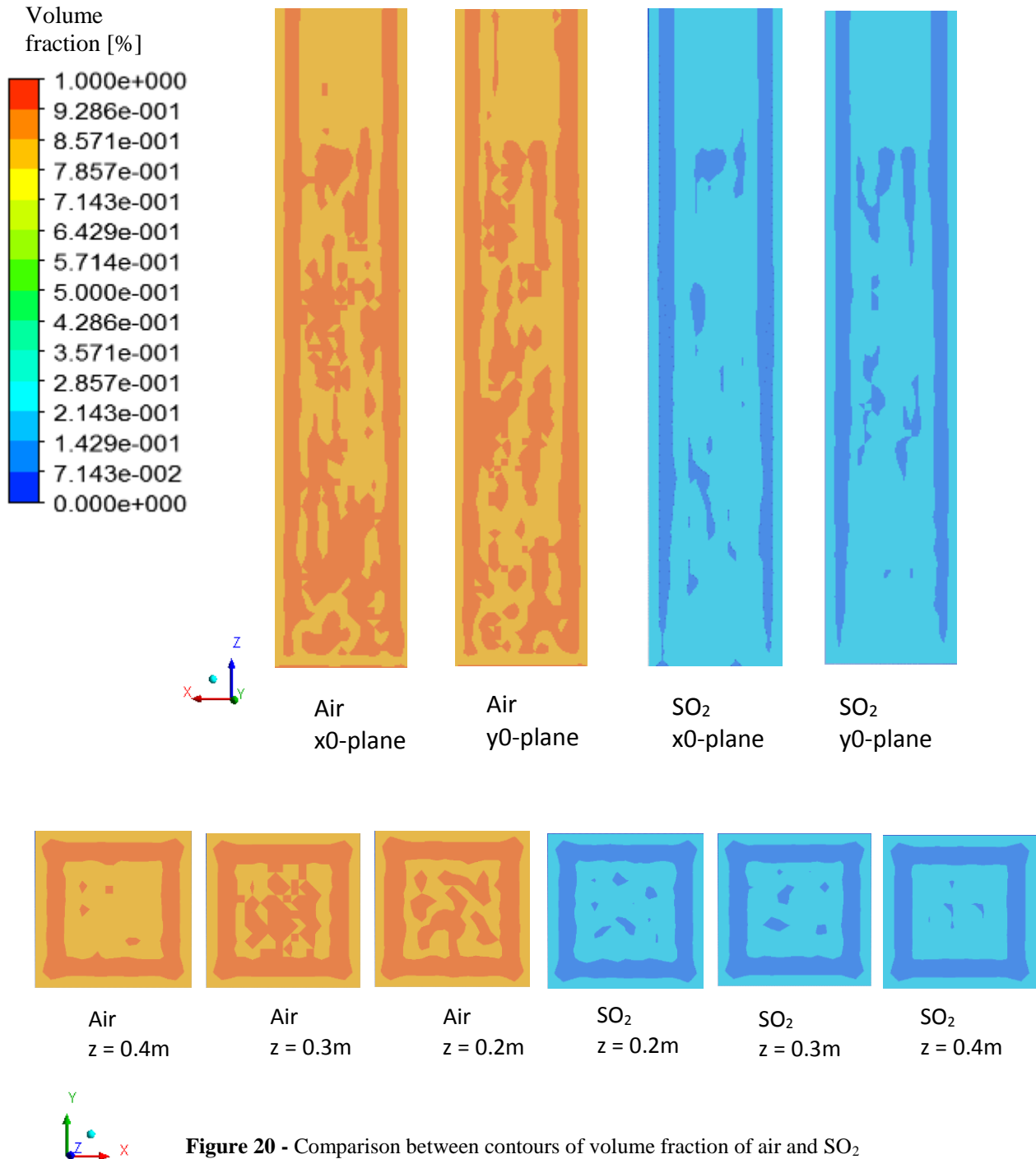
Volume fraction of air and SO₂ for continuous phase with discrete particles, fig. 20, shows different symmetry as compared with that of the continuous phase, fig. 16. This effect can be caused by the injected particles which tend to disturb the symmetry of flow.

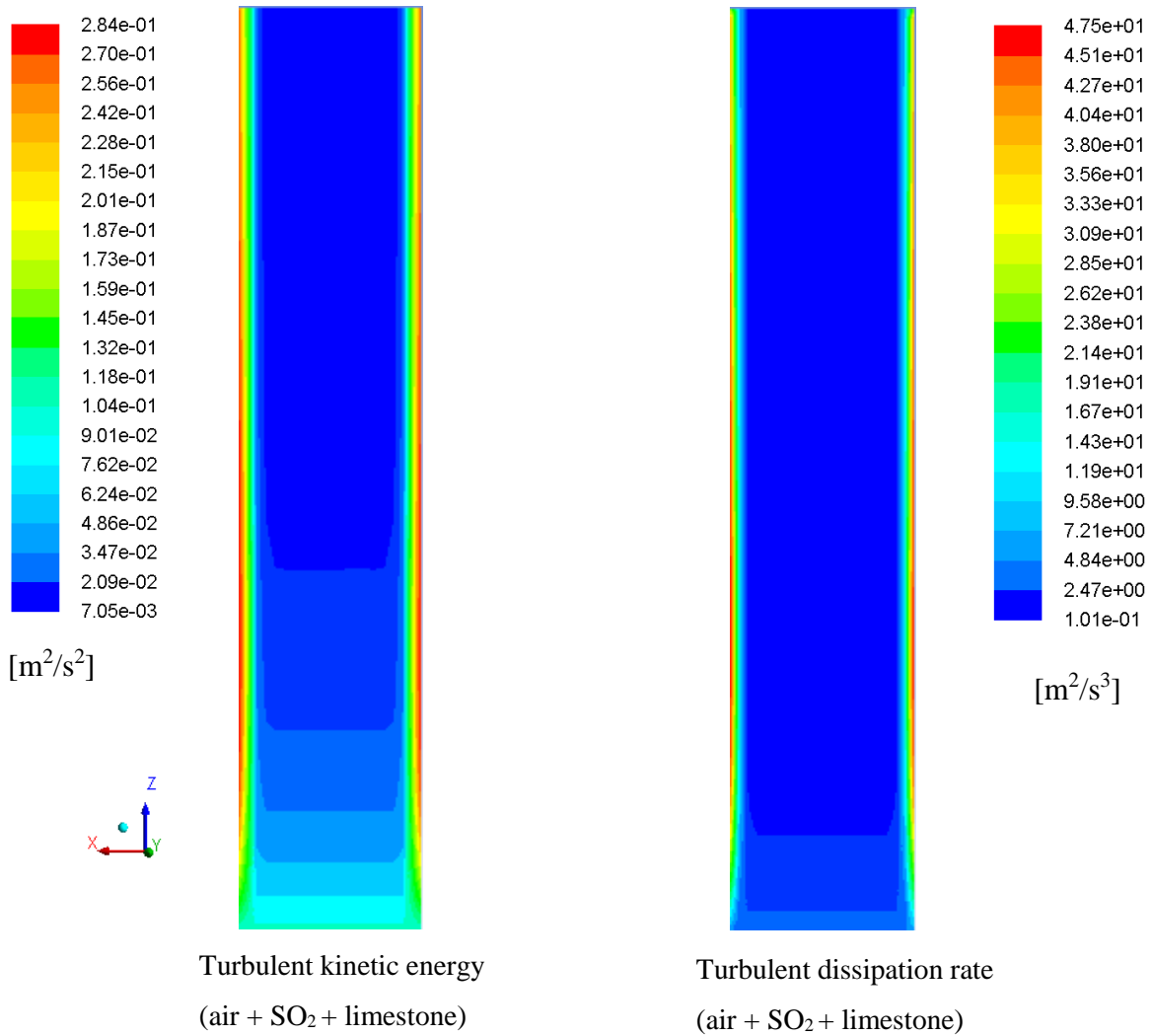|	
2.84e-01	4.75e+01
2.70e-01	4.51e+01
2.56e-01	4.27e+01
2.42e-01	4.04e+01
2.28e-01	3.80e+01
2.15e-01	3.56e+01
2.01e-01	3.33e+01
1.87e-01	3.09e+01
1.73e-01	2.85e+01
1.59e-01	2.62e+01
1.45e-01	2.38e+01
1.32e-01	2.14e+01
1.18e-01	1.91e+01
1.04e-01	1.67e+01
9.01e-02	1.43e+01
7.62e-02	1.19e+01
6.24e-02	9.58e+00
4.86e-02	7.21e+00
3.47e-02	4.84e+00
2.09e-02	2.47e+00
7.05e-03	1.01e-01

$[m^2/s^2]$　　　　　　　　　　　　　　　　$[m^2/s^3]$

Turbulent kinetic energy　　　　　Turbulent dissipation rate

$(air + SO_2 + limestone)$　　　　　$(air + SO_2 + limestone)$

Figure 21 - Turbulence kinetic energy and dissipation rate of the mixture for continuous phase

The turbulent kinetic energy and dissipation rate for continuous phase with discrete particles is similar to that of continuous phase. The explanation is because the inert particles of limestone have effected the turbulence in very small quantities.

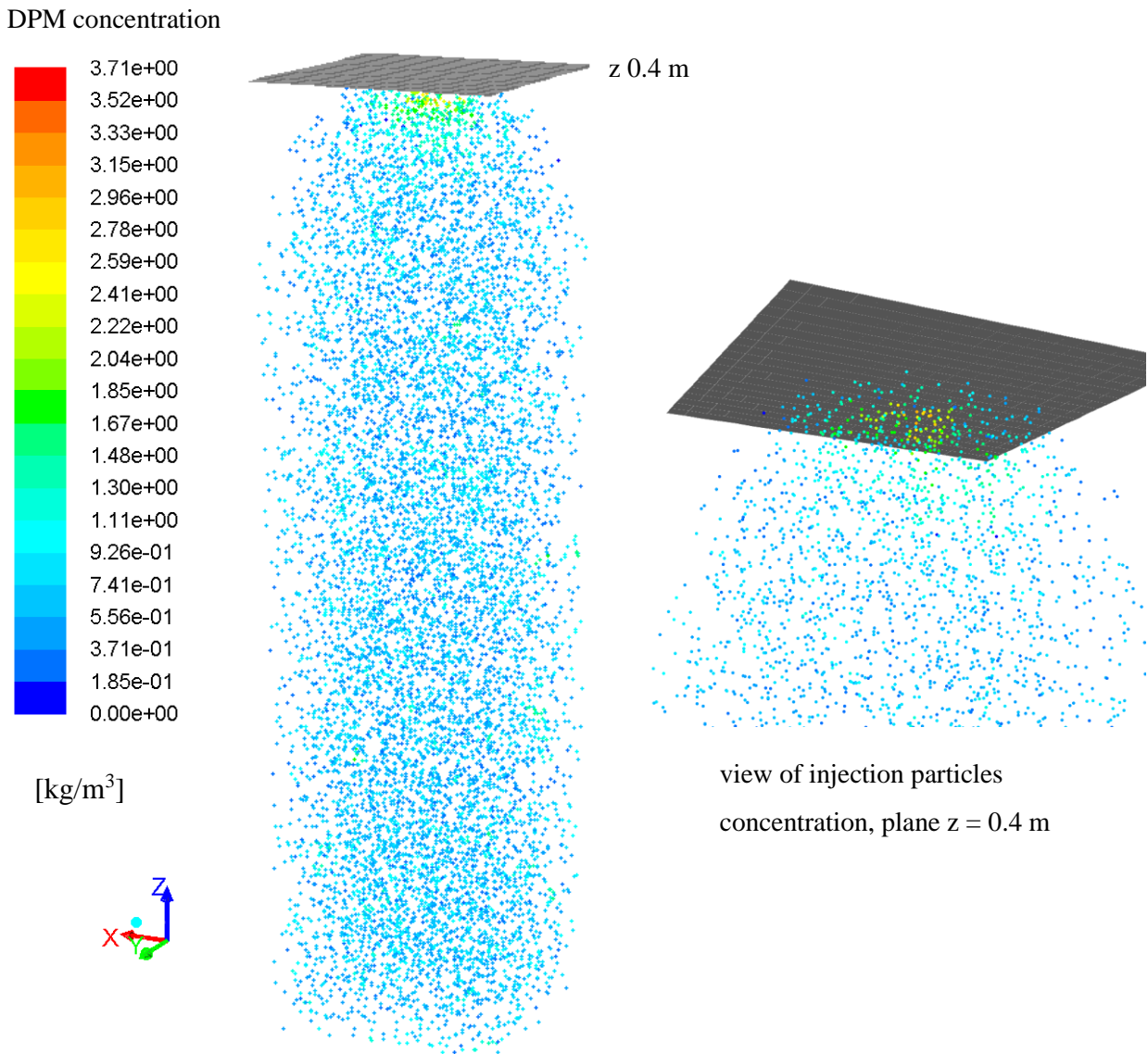*Contours of discrete phase concentration (concentration of particles);*
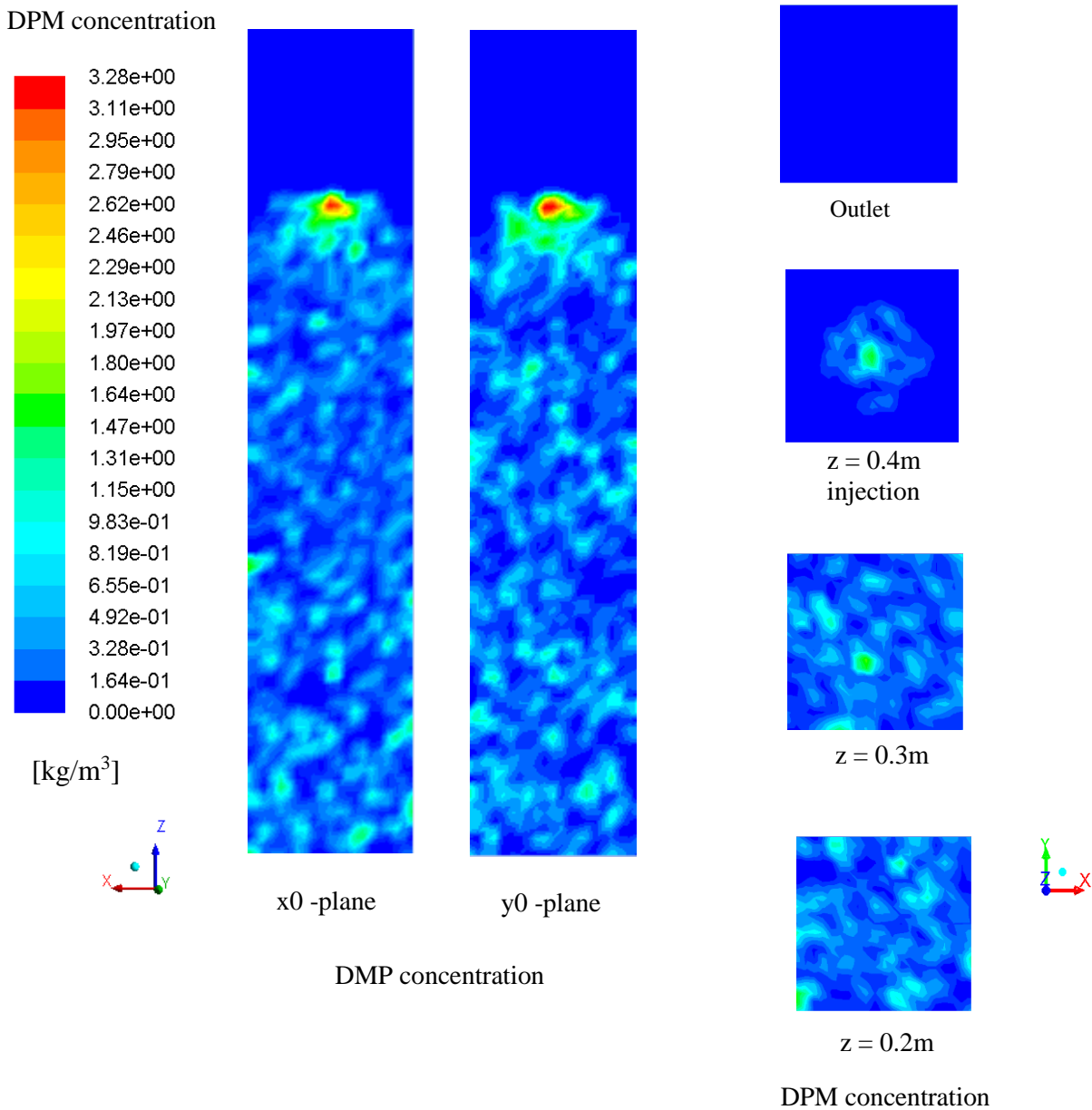
Figure 22 – Contours of discrete phase concentration

Since the flow is transient, from the Figure 22 we can see the concentration of sprayed particles from the injection point, in which point the concentration is higher at the injection zone. From the x0 plane it can be seen the shape of spray cone from the injection point.

Particle traces colored by discrete phase concentration;

DPM concentration

3.71e+00	
3.52e+00	
3.33e+00	
3.15e+00	
2.96e+00	
2.78e+00	
2.59e+00	
2.41e+00	
2.22e+00	
2.04e+00	
1.85e+00	
1.67e+00	
1.48e+00	
1.30e+00	
1.11e+00	
9.26e-01	
7.41e-01	
5.56e-01	
3.71e-01	
1.85e-01	
0.00e+00	

$[kg/m^3]$

z 0.4 m

view of injection particles
concentration, plane z = 0.4 m

Figure 23 – Particles traces colored by DPM concentration and the z = 0.4 plane of injection

From the fig. 23 it is shown the concentration of traced particles of limestone through the computational domain. The concentration has maximum value in some small region near the injection point, and the spread particles has symmetry of distribution as will be shown in fig. 24.

Symmetry of injected particles colored by discrete phase concentration;

DPM concentration

■	3.71e+00
	3.52e+00
	3.33e+00
	3.15e+00
	2.96e+00
	2.78e+00
	2.59e+00
	2.41e+00
	2.22e+00
	2.04e+00
	1.85e+00
	1.67e+00
	1.48e+00
	1.30e+00
	1.11e+00
	9.26e-01
	7.41e-01
	5.56e-01
	3.71e-01
	1.85e-01
■	0.00e+00

[kg/m^3]

y0 plane

x0 plane

injection point
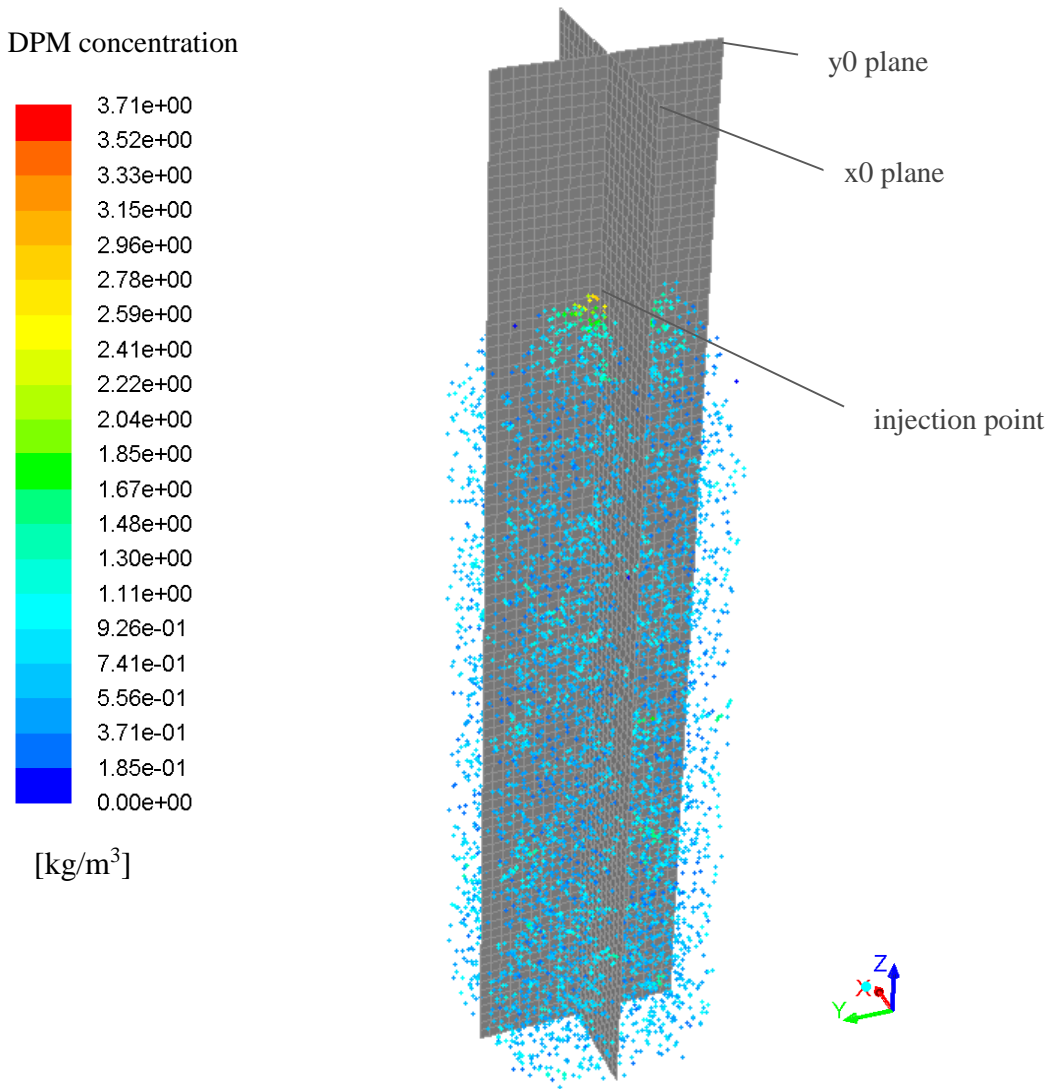
Figure 24 – Particle traces colored by DPM concentration in x0 and y0 planes

DPM concentration in fig. 24 shows the same information as fig. 23, in which now the planes of symmetry are added and it can be seen the distribution of limestone particles around the planes x0 and y0. From the figures, 22, 23, and 24, we can notice that there are no particles above the injection zone to outlet, and this shows that the particles are falling down because of the gravity.

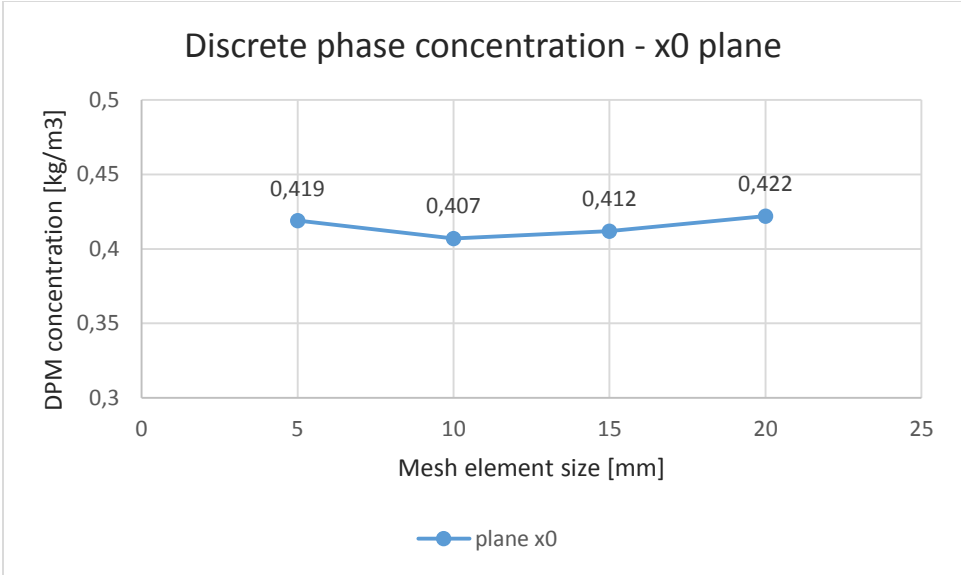| Finite volume elements (grid)	Size of elements	No. of elements
Very coarse	20 mm	625
Coarse	15 mm	1617
Medium	10 mm	5000
Fine	5mm	39200

Table 4 – Finite volume element parameters
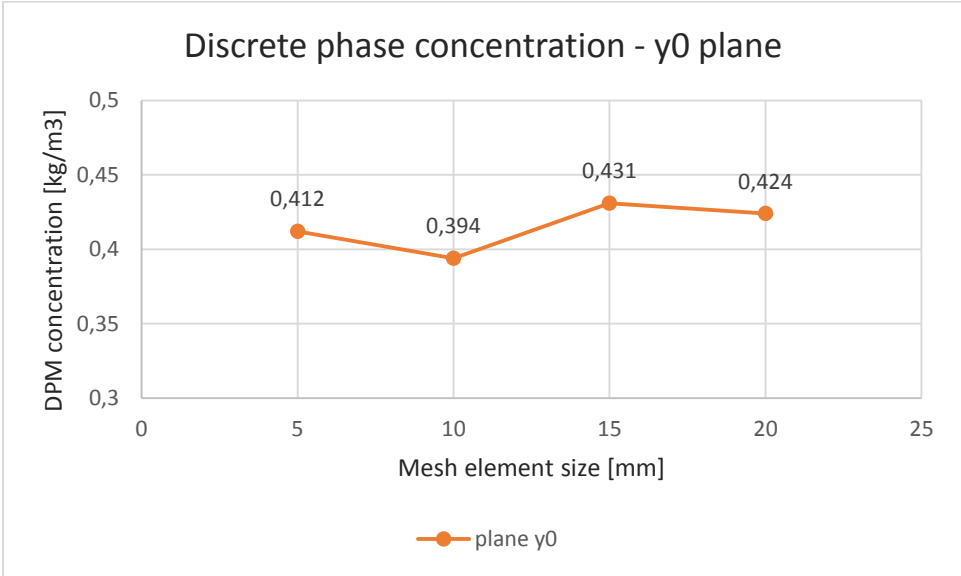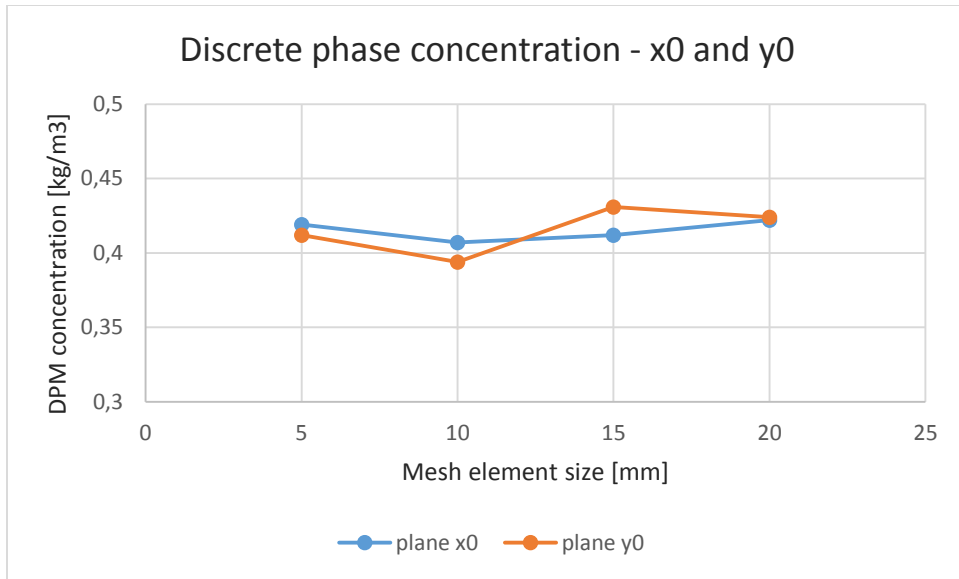

Figure 25 – DPM concentration in x0 plane

Figure 26 – DPM concentration in y0 plane

Figure 27 – DPM concentration in x0 and y0 planes
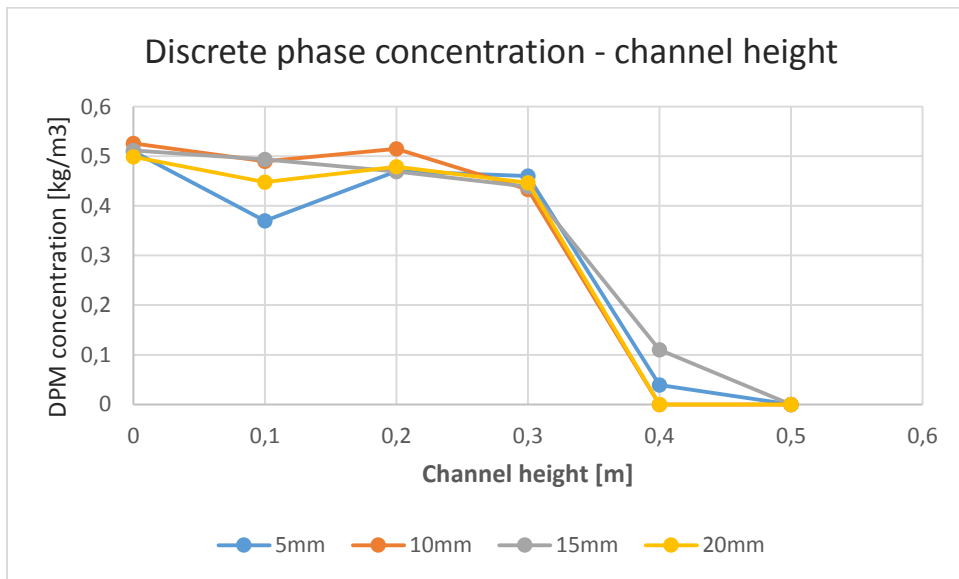
Figure 28 – DPM concentration with channel height

According to the height of the channel, planes of measurement for concentration of discrete phase showed in the chart in fig.28 are; 0 (Inlet), $z = 0.1$, $z = 0.2$, $z = 0.3$, $z = 0.4$ (injection point), $z = 0.5$ (Outlet).

Three more different domain discretization with element size, 10 mm, 15 mm, and 20 mm, as described from table 4 have been simulated with the same initial conditions as for the continuous

and discrete phase simulation with element size 5 mm. The data from simulations obtained by surface integrals of area weighted average for the planes mentioned above, were evaluated in excel and the charts from results are shown in fig. 25-28. From the results of discrete phase concentrations in plane x0 and y0, for the four domain discretization, we can conclude that batter symmetry of concentration have the domain with 5 and 20 mm size of elements. Even though, also the other two domains with 10 mm and 15 mm, can be seen as with small changes in concentration if we compare to the size of the channel.

The results from the fig. 28 show the concentration of discrete phase with the height of the channel. As it is seen from the chart, the four discretization domains have similar trends of results. The concentration of discrete phase at the outlet is zero for the four domains, and increases with decreasing in height of the channel.

Chapter 5: Evaluation and discussion of the results

The intention of this work was to define material and physical model for the numerical simulation of the flow and chemical reactions in the absorber for desulfurization of flue-gas, and compare the results with experiment or work of other authors.

The two parts dealing with material and physical model was investigated thoroughly, which include the evaluation of the material properties for the laboratory scaled scrubber, the definition of the spray injection parameters, proper scaling of the input data, and the physical model for the flow of flue gas and limestone inert particles.

The data of flue-gas and limestone particles for simulation of the flow with chemical reactions through the channel were introduced into the software. These data were obtained from different books and latest articles publications dealing with wet flue-gas desulfurization process as mentioned in the chapter 3. Figure 8.

In this work the scrubber geometry was simplified for the reasons of qualitative investigation rather than quantitative.

From the results achieved in this work the fluid dynamics inside the channel can be described as a gas-solid two-phase flow consisting of a carrier gas and a large number of dispersed particles and it was modeled with Euler-Lagrange approach.

To model all of the equations mentioned for the chemical reaction of SO_2 and droplets of limestone it is a complicated process and requires correct input data of the coefficients included in the reaction. In this work it is used only continuity, momentum and energy equations for the continuous phase and discrete phase without additional source terms. In this way we can model different quantities of the problem which can show some insight about the flow between flue-gas and particles of limestone. The quantities that can be modeled are: velocity profiles and temperature distribution, concentration of continuous and discrete phase, turbulence kinetic energy and dissipation rate of the mixture, the percentage of concentration for the limestone particles and the diffusivity of the limestone particles in the continuous phase.

From the velocity profiles of continuous phase in the first simulation, and velocity profiles of continuous phase with added particles of limestone in the second simulation, we can see only minor change in velocity magnitude. From the first simulation of continuous phase, this is explained in simple terms, and it has to be with the fluid flow which passes through a rectangular

shape channel which encounters obstacle only by the channel wall because of friction forces. In the other part of the channel the flow is uniform and it shows symmetry in both orthogonal planes.

In the other hand, from the second simulation of continuous phase with added inert particles of limestone, the small changes of velocity magnitude of the gas is explained by the fact that inert particle of limestone are present in the flow with opposite direction. This particles are very small in diameter (0.001m), and as a consequence their impact in the flue-gas is very small. A small decrease in velocity magnitude that can be noticed, is in the bottom part of the channel which can be effected by the increased concentration of the discrete particles as illustrated from the chart of DPM concentration in Figure 28 . In this section, the streamlines of gas flow tends to diverge from their path by passing around the particles which leads to a very small decreases of the total velocity magnitude.

Because of the complexity of modeling two phase flow with discrete particles the last step of the simulations which deals with modeling of chemical reaction between sulfur dioxide and limestone slurry was not finalized. This requires exact evaluation of parameter and chemical coefficients which can be achieved only by experimental measurements. I think that it has been prepared a solid introductory through the literature review about the chemical reactions process, and the future work of different researchers can rely and maybe find helpful information on the presented work.

The symmetry of the flow shown from the velocity contours of continuous phase in x0 and y0 planes, tells an important role, since the further investigations in this field can be done only by using the quarter of the model.

References

[1] K. Brown, W. Kalata and R. Schick, "Optimization of SO2 Scrubber using CFD Modeling," *Elsevier Ltd.,* pp. 170-180, 2013.

[2] R. M. Beychok, Couping with SO2, Chemical Engineering/Deskbook Issue, 1974.

[3] H. Brauer and Y. B. Varma, Air Pollution Control Equipment, Berlin: Springer-Verlag, 1981.

[4] J. Katolicky and M. Jicha, "Influence of the Lime Slurry Droplet Spectrum on the Efficiency of Semi-Dry Flue Gas Desulfurization," *Chemical Engineering Technology ,* vol. 1, no. 36, pp. 156-166, 2013.

[5] M. Walsh, "Wet FGD Types and Fundamentals," Marsulex Environmental Technologies , 2008.

[6] R. K. Srivastava, "Controlling SO2 emissions: A review of technologies," National Risk Management Research Laboratory, Washington, DC, 2000.

[7] L. Marocco and F. Inzoli, "Multiphase Euler–Lagrange CFD simulation applied to Wet Flue Gas Desulphurisation technology," *International Journal of Multiphase Flow,* pp. 185-194, 2009.

[8] Q. Wen, X. Y, G. Zeng, C. T. Li, S. Li, G. Guo and J. Song, "Optimal design of a wet-type desulphurization absorber by the numerical simulation method," *Chemical Engineering Research and Design,* vol. 92, no. 7, pp. 1257-1266, 2014.

[9] B. Buecker, "Gypsum Seed Recycle in Wet-Limestone Scrubbers," *unpublished paper presented at the Utility Representatives FGD Conference,* 1986.

[10] J. Warych and M. Szymanovwski, "Model of the Wet Limestone Flue Gas Desulphurization Process for Cost Optimization," *Industrial & Engineering Chemistry Research ,* vol. 40, no. 12, pp. 2597-2605, 2001.

[11] Ansys, Inc., "Fluent User´s Guide Release 15.0," November 2013. [Online]. Available: www.ansys.com. [Accessed 1 October 2015].

[12] J. Delgadillo and J. Rajmani, "A comparative study ofthree turbulence-closure models for the hydrocycloneproblem," *Int. J. Miner,* vol. 77, pp. 217-230, 2005.

[13] B. V. Vivek, D. S. Deo and R. V. Vivek, "Eulerian–Lagrangian simulations of unsteady gas–liquid flows in bubble columns," *International Journal of Multiphase Flow,* vol. 32, no. 7, pp. 864-885, 2006.

[14] B. Wang, K. Chu and A. Yu, "Numerical Study of Particle−Fluid Flow in a Hydrocyclone," *Industrial & Engineering Chemistry Research,* vol. 46, no. 13, pp. 4695-4705, 2007.

[15] B. E. Launder and B. D. Spalding, Lectures in mathematical models of turbulence, London: Academic Press, 1972.

[16] C. T. Crowe, J. D. Schwarzkopf, M. Sommerfeld and Y. Tsuji, Multiphase flows with droplets and particles, Boca Raton: CRC Press, 2011.

[17] A. Bes, Dynamic Process Simulation of Limestone Calcination in Normal Shaft Kilns,, Fakultät für Verfahrens- und Systemtechnik der Otto-von-Guericke-Universität Magdeburg, 2005.

[18] J. Xu, P. y. Liu, M. Zeng and Q. w. Wang, "Numerical Study on the Effects of Flue-Gas Inlet Type for the Flue-Gas-Desulfurization Wet Scrubber," *Chemical Engineering Transactions,* vol. 21, pp. 241-246, 2010.

[19] J. Novosád and T. Vít, "Numerical simulation of flow in the wet scrubber for desulfurization," *EPJ Web of Conferences,* vol. 92, 2015.

[20] N. Isabella, C. Ciardelli, E. Tronconi, D. Chatterjee and B. Bandl-Konrad, "NH3-SCR of NO over a V-based catalyst: Low-T redox kinetics with NH3 inhibition," *AIChE Journal,* vol. 52, no. 9, pp. 3222-3233, 2006.